

Thermodynamic Modeling of Ionic Liquid Systems: Development and Detailed Overview of Novel Methodology Based on the PC-SAFT

Kamil Paduszyński* and Urszula Domańska

Department of Physical Chemistry, Faculty of Chemistry, Warsaw University of Technology, Noakowskiego 3, 00-664 Warsaw, Poland

S Supporting Information

ABSTRACT: We present the results of an extensive study on a novel approach of modeling ionic liquids (ILs) and their mixtures with molecular compounds, incorporating perturbed-chain statistical associating fluid theory (PC-SAFT). PC-SAFT was used to calculate the thermodynamic properties of different homologous series of ILs based on the bis(trifluoromethylsulfonyl)imide anion ($[\text{NTf}_2]$). First, pure fluid parameters were obtained for each IL by means of fitting the model predictions to experimental liquid densities over a broad range of temperature and pressure. The reliability and physical significance of the parameters as well as the employed molecular scheme were tested by calculation of density, vapor pressure, and other properties of pure ILs (e.g., critical properties, normal boiling point). Additionally, the surface tension of pure ILs was calculated by coupling the PC-SAFT equation of state with density gradient theory (DGT). All correlated/predicted results were compared with literature experimental or simulation data. Afterward, we attempted to model various thermodynamic properties of some binary systems composed of IL and organic solvent or water. The properties under study were the binary vapor–liquid, liquid–liquid, and solid–liquid equilibria and the excess enthalpies of mixing. To calculate cross-interaction energies we used the standard combining rules of Lorentz–Berthelot, Kleiner–Sadowski, and Wolbach–Sandler. It was shown that incorporation of temperature-dependent binary corrections was required to obtain much more accurate results than in the case of conventional predictions. Binary corrections were adjusted to infinite dilution activity coefficients of a particular solute in a given IL determined experimentally or predicted by means of the modified UNIFAC (Dortmund) group contribution method. We concluded that the latter method allows accurate and reliable calculations of bulk-phase properties in a totally predictive manner.



INTRODUCTION

In the last two decades, ionic liquids (ILs) have received a lot of attention in different fields of pure and applied chemistry, including chemical engineering and separations,^{1,2} biotechnology,³ synthesis and catalysis,^{4,5} and electrochemistry.^{6,7} Due to their unique physical characteristics such as low melting point, extremely low vapor pressure, as well as high thermal, chemical, and electrochemical stability, the ILs are considered as potential “green” replacements for conventional volatile organic solvents in sustainable designing of modern and clean processes. There is no doubt that utilization of processes involving ILs will significantly reduce exposure of toxic and harmful chemicals to the environment. Moreover, ILs disclose a great solvating capacity and selectivity for a variety of inorganic⁸ and organic materials, including pharmaceuticals⁹ and biomass (carbohydrates,^{10,11} lignins,¹² or other biomass feedstock for production of biofuels, e.g., *Miscanthus*¹³). Therefore, possible utilities of ILs in future technologies based on the concept of biorefinery have attracted a lot of attention.¹⁴

The most essential feature of ILs is their “tunability”, and hence, the ILs are often referred as “designer solvents”. This is due to practically innumerable possible combinations of ions that can be synthesized and functionalized for specific tasks. Diverse physical and chemical properties of ILs due to cation/

anion (e.g., density, viscosity, polarity, solubility) can be easily tailored by their chemical structures, e.g., alkyl chain length attached to the cationic/anionic core. Of course, trial and error methods are impractical for selection of a suitable IL for a particular application. It is essential from the point of view of physical chemistry and solution thermodynamics to understand the ILs at the molecular level and get more physical insight into their unique physical and chemical properties.^{15,16} Therefore, development of theoretical approaches allowing accurate modeling of IL-based systems is crucial. Nevertheless, the complexity of such systems at the molecular scale poses an important obstacle to effective modeling and makes the problem very difficult and challenging.

Thus far, several theoretical as well as empirical approaches have been adopted to reproduce experimental data on the thermodynamic properties of pure ILs and multicomponent mixtures containing ILs: simple and more elaborated group contributions models,^{17,18} conventional cubic equations of state,¹⁹ activity coefficient models,^{20–22} lattice theory,^{23–27} equation of state for square-well chain fluids with variable well-width range

Received: January 28, 2012

Revised: March 28, 2012

Published: April 2, 2012

(SWCF-VR),²⁸ and the whole family of models based on statistical associating fluid theory (SAFT): perturbed-chain SAFT (PC-SAFT),^{26,27,29} variable-potential range SAFT (SAFT-VR),²⁹ truncated PC-SAFT (tPC-SAFT),^{30,31} soft-SAFT,^{32–34} and heterosegmented SAFT.^{35,36} A comprehensive overview of the state of the art in the field of modeling of ILs-based systems was provided by Vega and co-workers.³⁷ Besides simple models, more sophisticated computational techniques were successfully applied as well. Those methods are molecular dynamics and Monte Carlo simulations^{38–43} and quantum mechanics-based COSMO-RS.⁴⁴ Although they are based on well-established foundations and provide realistic molecular models reflecting many characteristic features of ILs, their usage requires a lot of experience, specialist software, etc. Moreover, the calculations are usually not straightforward, time consuming, and expensive. In practical applications, however, a compromise on the accuracy, reliability, simplicity, time, and cost of calculations must be hammered out. It suggests an application of simpler models, such as equations of state.

In our laboratory we deal with experimental investigations and modeling of systems composed of ILs and molecular compound(s) in terms of various empirical as well as theoretical models. Recently, we turned our attention to PC-SAFT^{45–47} and used this approach to model binary liquid–liquid equilibrium (LLE) phase diagrams of mixtures composed of hydrocarbons, alcohols, or water and ILs based on 1-alkyl-1-methylpiperidinium cation and bis(trifluoromethylsulfonyl)-imide anion, $[C_nC_1Pip][NTf_2]$, where alkyl = *n*-propyl (*n* = 3) or alkyl = *n*-butyl (*n* = 4).^{26,27} LLE in systems $\{[C_3C_1Pip][NTf_2] + \text{alcohol}\}$ were calculated in the conventional manner.²⁶ First, PC-SAFT pure fluid parameters were obtained by fitting the model predictions to experimental liquid density and Hildebrand's solubility parameters of the IL determined from infinite dilution data. Then, the classical combining rules were adopted and the LLE phase diagrams calculated. Unfortunately, the model did not predict phase splitting in the systems studied. To resolve this problem, temperature-dependent binary interaction parameters correcting the Lorentz–Berthelot rules were introduced and a satisfactory description of the experimental data was provided.²⁶ The main disadvantage of this way of modeling is that it is not predictive. To overcome this limitation we followed the work of Schacht et al.⁴⁸ and proposed application of experimental activity coefficients at infinite dilution of molecular solutes in ILs (γ^∞) for correlation of binary interaction parameters.²⁷ This method is not purely predictive as well. However, the γ^∞ data used to obtain binary corrections are much easier to measure than LLE phase diagrams or other bulk-phase properties of binary systems at finite concentrations. The results of liquid–liquid equilibria in binary systems $\{[C_3C_1Pip][NTf_2]$ or $[C_4C_1Pip][NTf_2] + n\text{-alkane}$ or cycloalkane $\}$ were in good agreement with experimental data. The accuracy of predictions was satisfactory and substantially improved compared with conventional predictions.²⁷ Therefore, one could treat this work as a step forward in the development of the predictive PC-SAFT approach for ILs.

In this contribution we summarize development and testing of novel methodology for calculating bulk-phase thermodynamic properties of binary systems containing ILs. The proposed methodology is similar to that reported by us previously²⁷ and rests on application of infinite dilution data to describe binary interaction parameters involved in the PC-SAFT combining rules. This time, however, we present a totally predictive methodology as the utilized γ^∞ values are calculated with modified UNIFAC (Dortmund),^{18,49,50} which is nowadays

the most reliable and versatile group contribution method for predicting the γ^∞ data. Furthermore, our previous papers were focused only on liquid–liquid equilibrium and piperidinium ILs. In turn, the results presented in this work comprise calculations of vapor–liquid, liquid–liquid, and solid–liquid equilibria (VLE, LLE, and SLE, respectively) and excess enthalpies of mixing (H^E). Moreover, calculations are presented for a greater number of binary systems composed of $[NTf_2]$ -based ILs belonging to different cation families, namely, imidazolium, pyridinium, pyrrolidinium, and piperidinium.

The rest of the paper is organized as follows. First, we summarize the main theoretical aspects of the work, including a brief description of the models used and detailed presentation of the new methodology. Then, the results of calculations are presented and discussed for the pure ILs and the binary systems. Finally, some remarks and conclusions are recapitulated in the last section.

THEORY

PC-SAFT Equation of State. Perturbed-chain statistical associating fluid theory (PC-SAFT)^{45–47} is an approach based on Wertheim's thermodynamic perturbation theory,^{51–54} which was derived from the statistical mechanics of molecular chains composed of spherical segments interacting by short-range physical (dispersion) and/or highly directional specific forces (association, e.g., hydrogen-bonded systems). In terms of PC-SAFT, hard-chain fluid serves as a reference for the perturbation expansion. This is in contrast to original SAFT developed by Chapman et al.,⁵⁵ where hard-sphere fluid was employed. The thermodynamics of a mixture is expressed as a dependence of residual Helmholtz free energy (A^{res}) on temperature, number density, and composition. Contributions to free energy due to hard-chain formation (hc), dispersive interactions (disp), dipole–dipole interactions (polar), and association (assoc) are taken into account explicitly

$$\tilde{a}^{\text{res}} \equiv \frac{A^{\text{res}}}{Nk_B T} = \tilde{a}^{\text{hc}} + \tilde{a}^{\text{disp}} + \tilde{a}^{\text{polar}} + \tilde{a}^{\text{assoc}} \quad (1)$$

In eq 1 *N* stands for the number of molecules in the system and k_B is the Boltzmann constant. In this paper we will not discuss all of the PC-SAFT equations in detail. A comprehensive summary and derivation of all expressions involved in eq 1 can be found elsewhere.^{45–47} In this section we only introduce the model parameters and combining rules.

In the case of systems that contain only nonassociating and nonpolar components (e.g., hydrocarbons, noble gases), only the first two terms need to be included in eq 1. Each component of such a mixture is described by three characteristic pure-fluid parameters: the number of spherical segments forming the chain (*m*), hard-sphere segment diameter (σ), and dispersion energy potential well depth (u/k_B). To account for dipole–dipole interactions present in polar components such as ketones or ethers (i.e., to make a transition from the PC-SAFT to the PC Polar-SAFT model, PCP-SAFT), a “polar” term is needed in eq 1. Thus far, several terms have been reported in the literature. The most popular are those proposed by Jog and Chapman,⁵⁶ Karakatsani,⁵⁷ and Gross and Vrabec.⁴⁷ In this work, the Gross–Vrabec term is utilized as it utilizes only permanent dipole moments of molecules and there are no other adjustable parameters required. For systems composed of at least one associating component (e.g., water, alcohol, carboxylic acid), an association contribution in eq 1 becomes the most

essential from the point of view of the thermodynamic behavior of the system. Such an associating system is additionally characterized by the presence of different types of associating sites attached to molecules. To characterize a given specific interaction between site A and site B, two additional parameters describing the strength of association are introduced. Those parameters are the energy potential well depth and the volume of association, denoted by ε^{AB}/k_B and κ^{AB} , respectively.

In summary, any pure substance is described by three or more PC-SAFT parameters depending on its chemical nature. A common procedure for calculating all those parameters rests on adjusting them to experimentally pure substance properties, such as the saturated liquid and/or vapor density or vapor pressure. The experimental data used in the regression are usually taken from DIPPR data compilations⁵⁸ and cover a broad range of temperature, for instance, 0.5–0.9 of reduced temperature.⁵⁹ Nevertheless, it should be pointed out that new procedures for determination of the PC-SAFT parameters were recently developed. In particular, Albers and Sadowski⁶⁰ proposed the PCP-SAFT parameter calculation procedure based on a minimal set of experimental liquid density or vapor pressure data. Furthermore, Ferrando et al.⁶¹ elaborated a novel methodology to determine the PC-SAFT association scheme and association parameters for linear alcohols with Monte Carlo simulations. In turn, the procedure for calculation of force field parameters based on the PC-SAFT results was studied as well and illustrated by optimizing transferable Lennard–Jones parameters for the *n*-alkane series.⁶²

In order to apply the PC-SAFT equations to mixtures, one needs to assume combining rules for cross-interaction parameters involved in the dispersion and association terms. The potential well depth for dispersive interactions of segments constituting different molecules *i* and *j* (i.e., u_{ij}/k_B) as well as the segment diameter corresponding to this interaction (i.e., σ_{ij}) are usually calculated by using the well-known quadratic combining rules of Lorentz–Berthelot (LB)

$$u_{ij} = \sqrt{u_i u_j}, \quad \sigma_{ij} = \frac{\sigma_i + \sigma_j}{2} \quad (2)$$

In the case of associating systems, two kinds of mixtures, differing in association scheme, can be encountered. The first type comprises cross-associating systems, such as mixtures of alcohols, amines, carboxylic acids, or water. In such systems, associating site A on molecule *i* (A_i) can interact with associating site B on molecule *j* (B_j). At the same time, associating site B on molecule *i* (B_i) can interact with associating site A on molecule *j* (A_j). To calculate the energy and volume of the cross-association (namely, $\varepsilon^{A_i B_j}/k_B$, $\varepsilon^{A_j B_i}/k_B$, and $\kappa^{A_i B_j}$, $\kappa^{A_j B_i}$), appropriate combining rules are required. It was found that the following relations proposed by Wolbach and Sandler (WS)⁶³ are suitable to describe the effects related to cross-association when coupled with SAFT-based models

$$\begin{aligned} \varepsilon^{A_i B_j} &= \varepsilon^{A_i B_i} \\ &= \frac{\varepsilon^{A_i B_i} + \varepsilon^{A_j B_j}}{2} \\ \kappa^{A_i B_j} &= \kappa^{A_i B_i} \\ &= \sqrt{\kappa^{A_i B_i} \kappa^{A_j B_j}} \left(\frac{2\sqrt{\sigma_i \sigma_j}}{\sigma_i + \sigma_j} \right)^3 \end{aligned} \quad (3)$$

The second type of associating systems is a mixture composed of self-associating compound(s) *i* and at least one polar compound *j*, which is not self-associating. Molecules of component *j* possess, however, functional groups which can act as either acceptors or donors in specific interactions. An example of this kind of system is an aqueous solution of a ketone, in which lone pairs of electrons in the oxygen atom constituting the carbonyl group of the ketone (site B_j) can play the role of acceptors for the hydrogen atoms of water molecules acting as donor sites (site A_i). Equation 3 cannot be plainly applied for this kind of cross-association since the self-association does not occur in a pure ketone, and hence, some simplifying assumptions have to be made to account for $A_i B_j$ cross-association and respective PC-SAFT parameters. A simple approach to take into account this “induced” association was proposed by Kleiner and Sadowski,⁶⁴ who stated that one can apply the WS combining rules provided that the energy parameter for pure not associating components is set to zero, while the association volume is the same as the corresponding parameter for the self-associating compound. Then

$$\varepsilon^{A_i B_j} = \frac{\varepsilon^{A_i B_i}}{2}, \quad \kappa^{A_i B_j} = \kappa^{A_i B_i} \left(\frac{2\sqrt{\sigma_i \sigma_j}}{\sigma_i + \sigma_j} \right)^3 \quad (4)$$

The former assumption is quite obvious, whereas the latter one follows from the fact that the accuracy of the phase behavior description in terms of PC-SAFT is less sensitive toward this parameter. Moreover, the predictive ability of the model is preserved, because there is no additional adjustable parameter(s) depending on the kind of polar compound *j*.⁶⁴ We will refer to eq 4 as Kleiner–Sadowski (KS) combining rules.

Finally, if pure fluid parameters are known for all components forming the mixture, the PC-SAFT equations combined with eqs 2–4 can be used in an entirely predictive manner. However, satisfactory results can be obtained only for systems composed of a fairly similar size and chemical nature. To overcome this obstacle, binary interaction corrections to energetic cross-interaction parameters of LB, WS, and KS combining rules (denoted by k_{ij}^{LB} , k_{ij}^{WS} , and k_{ij}^{KS} , respectively) are introduced in accordance to the following definitions

$$u_{ij} = \sqrt{u_i u_j} (1 - k_{ij}^{LB}) \quad (5)$$

$$\varepsilon^{A_i B_j} = \frac{\varepsilon^{A_i B_i} + \varepsilon^{A_j B_j}}{2} (1 - k_{ij}^{WS}) \quad (6)$$

$$\varepsilon^{A_i B_j} = \frac{\varepsilon^{A_i B_i}}{2} (1 - k_{ij}^{KS}) \quad (7)$$

The expressions for σ_{ij} and $\kappa^{A_i B_j}$ are assumed to be the same as in eqs 2–4. Of course, $k_{ii}^{LB} = k_{ii}^{WS} = k_{ii}^{KS} = 0$ and $k_{ii}^X = k_{ij}^X$, where superscript X stands for LB, WS, or KS. In the conventional equation-of-state modeling, the binary corrections are usually obtained from experimental binary data of interest by means of fitting. Such an approach results in vanishing of the predictive capabilities of the model, unless a distinct method for calculation of k_{ij}^X is available. Thus, development of either new methods and/or correlations for determination of the binary interaction parameters or totally new combining rules is very attractive.

It should be noted that this is the very first time when the WS and KS combining rules are used in the form given in eqs 6 and 7. Usually when cross-associating systems are described not in terms of purely predictive WS/KS combining rules, $\varepsilon^{A_i B_j}/k_B$ and/or $\kappa^{A_i B_j}$ parameters are treated as adjustable parameters as

themselves, e.g., as in the paper of Kleiner and Sadowski.⁶⁴ In this work, we decided to adopt this way of representation of cross-association parameters to make the thermodynamic description uniform for all types of mixtures.

Molecular Models. Prediction of thermodynamic properties of ILs-based systems with PC-SAFT requires a physically meaningful molecular model reflecting various characteristics of the constituting compounds. The PC-SAFT representation is quite straightforward for common molecular compounds such as hydrocarbons, ketones, alcohols, or water. Nevertheless, the problem is not obvious for ILs due to their complexity at the molecular level.¹⁵ Molecular simulations and small wide-angle X-ray scattering (SWAXS) experiments revealed that dispersive interactions as well as polar–electrostatic interactions,⁶⁵ ion pairing,^{66–69} and mesoscopic segregation^{70–75} have essential significance in those systems. Therefore, some simplifications have to be assumed to model such fluids with the PC-SAFT approach.

In this contribution we follow our previous works on modeling of ILs systems.^{26,27} According to the original idea, adopted from the work of Tsiptsias et al.,²⁵ ILs are pictured as being composed of neutral ion pairs while the interactions between ions due to Coulombic forces are identified as strong specific interactions. Although this methodology may be perceived as a controversial one, the use of associating sites in order to mimic the strong specific interactions in ILs can be justified by means of practical and physical arguments. The suggested approach substantially simplifies the calculations and is consistent with experimental and computational evidence on ion pairing in ILs.^{76,77} Moreover, an asymmetric charge distribution on the cation and delocalization of the electric charge due to the oxygen groups in the [NTf₂][−] anion result in electrostatic forces softening and generate highly directional interactions of shorter range, which can be depicted by the associating sites. The strength of the association can be adjusted by parameters $\epsilon^{\text{AB}}/k_{\text{B}}$ and κ^{AB} as well as by the number of positive (A) and negative (B) associating sites per ion pair. As in our previous works,^{26,27} we follow the paper of Tsiptsias et al.²⁵ and assume 5 positive sites A and 5 negative sites B per ion pair. The number of sites was selected to accurately reproduce experimental data on properties of pure ILs and their mixtures with a variety of organic solvents. Another goal was to develop the molecular model, allowing reliable estimation of vapor pressure of pure ILs based on pure fluid parameters obtained only from the temperature and pressure dependence of liquid density. In this work, we showed that the proposed 10-site model is suitable for this purpose. Moreover, we checked that much worse results of vapor pressure and binary phase equilibrium data are obtained when other molecular models are used (e.g., the 1-site model of Andreu and Vega³² or the 3-site model adopted by Llovel et al.³⁴).

Application of Limiting Activity Coefficients. Let us consider a binary mixture IL and molecular solvent denoted by 1 and 2, respectively. Then limiting the activity coefficients of 2 in 1 (γ_2^∞) can be calculated from the PC-SAFT equation of state using the following thermodynamic formula

$$\ln \gamma_2^{\infty, \text{SAFT}} = \ln \varphi_2^{L, \infty} - \ln \varphi_2^{L, 0} \quad (8)$$

where φ_2^L stands for the liquid phase fugacity coefficient of solute 2 in 1 and superscripts 0 and ∞ correspond to pure solute and solute infinitely diluted in the IL, respectively. On the other hand, the values of γ_2^∞ can be accessed by means of

the modified UNIFAC.^{18,50} Recently, application of infinite dilution data for determining binary interaction parameters of the PC-SAFT equation of state was proposed by Schacht et al.⁴⁸ The applicability of the method was demonstrated for a number of exemplary systems composed of polar or associating components and polymers. In our previous contribution,²⁷ we applied this methodology for a binary liquid–liquid equilibrium of systems {[C_nC₁Pip][NTf₂]} ($n = 3$ or 4) + hydrocarbons, alcohol, or water}. The binary interaction parameters of LB combining rules were assumed to be linearly dependent on temperature, namely, $k_{12}^{\text{LB}} = a_{12} + b_{12}(T/\text{K} - 298.15)$, while the k_{12}^{WS} parameter for {IL + alcohol or water} systems was set to be equal to zero (see eqs 5–7). Then the coefficients a_{12} and b_{12} were adjusted to experimental γ_2^∞ data. We showed that a significant improvement in accuracy can be obtained in comparison with traditional PC-SAFT predictions, i.e., when $k_{12}^{\text{LB}} = 0$.

In this work, we present a more detailed study on this methodology. First, the investigations comprise a greater diversity of cationic structures of ILs based on the [NTf₂][−] anion. This time, however, we attempted to develop a totally predictive method based on a combination of the PC-SAFT equation of state with the modified UNIFAC (Dortmund).^{18,50} The method rests on application of the PC-SAFT to describe bulk thermodynamic properties of pure ILs and their mixtures with a variety of organic solvents and water, while the modified UNIFAC is utilized to calculate limiting activity coefficients of a given solute in a specific IL ($\gamma_2^{\infty, \text{UNIFAC}}$). The following equation is solved with respect to k_{12}^{X} to obtain adequate binary corrections

$$\Phi(k_{12}^{\text{X}}, \gamma_2^{\infty, \text{UNIFAC}}) \equiv \gamma_2^{\infty, \text{SAFT}}(k_{12}^{\text{X}}) - \gamma_2^{\infty, \text{UNIFAC}} = 0 \quad (9)$$

In eq 9, X is set equal to LB, KS, or WS depending on the type of molecular component forming the binary system with IL. In particular, X = LB for {IL + hydrocarbon} mixtures in which cross-dispersion is the only kind of cross-interaction occurring in the system (corrections to LB combining rules, eq 5, are fitted to $\gamma_2^{\infty, \text{UNIFAC}}$ data); X = KS for {IL + polar molecular compound (e.g., ketone or ether)} mixtures, in which induced association occurs (corrections to KS combining rules, eq 6, are obtained from $\gamma_2^{\infty, \text{UNIFAC}}$ data, while k_{12}^{LB} is set to be equal to zero); X = WS for {IL + associating component (e.g., alcohol or water)} mixtures, in which cross-association plays a dominant role (k_{12}^{WS} are adjusted to $\gamma_2^{\infty, \text{UNIFAC}}$, whereas data binary cross-dispersion interactions are taken into account by classical LB combining rules, i.e., it is assumed that $k_{12}^{\text{LB}} = 0$). Please note that in our previous paper²⁷ we set $k_{12}^{\text{KS}} = k_{12}^{\text{WS}} = 0$ without regard to the type of solute. It means that for cross-associating systems, the binary corrections to the LB combining rules were considered as fitting parameters. Although the results were promising, we decided to update the methodology in the way described above to account for different types of systems and characteristic cross-interactions.

An important issue which should be also discussed is the temperature dependence of k_{12}^{X} (where X = LB, WS, KS). As a first approximation, one could assume the constant value of the corrections. It would significantly simplify calculations because of the requirement of only a single binary interaction parameter to obtain a complete thermodynamic description of a defined system. On the other hand, it was confirmed that more accurate predictions/correlations can be obtained when the temperature dependence of k_{12}^{X} is introduced to SAFT equations.^{26,30,31,36,78} In particular, one can use a polynomial to represent k_{12}^{X} data

obtained from thermodynamic properties at different temperatures. The actual $k_{12}^X(T)$ dependency can be, however, quite different than the assumed one, depending on the temperature range. In order to avoid ambiguity in the choice of $k_{12}^X(T)$ as well as the number and temperature range of γ_2^∞ data points involved in the fitting procedure, we assume that the temperature dependence of k_{12}^X is consistent with the temperature dependence of $\gamma_2^{\infty, \text{UNIFAC}}$ following from the modified UNIFAC predictions

$$\Phi[k_{12}^X(T); \gamma_2^{\infty, \text{UNIFAC}}(T)] = 0 \quad (10)$$

In further text, we will refer to the method based on eq 10 as PC-SAFT-UNIFAC.

Thus far, the modified UNIFAC parameter matrix is limited to ILs composed of imidazolium, pyridinium, and pyrrolidinium cations and three anions ($[\text{NTf}_2]$, $[\text{BF}_4]$, and $[\text{CF}_3\text{SO}_3]$).¹⁸ Interaction parameters are available for mixtures containing the ILs and alkanes, alkenes, cycloalkanes, aromatic hydrocarbons, ketones, THF, alcohols, and water.¹⁸ Fortunately, this set of parameters covers a great majority of the systems which will be discussed in this work. However, to adopt the presented methodology of calculating binary corrections to systems not represented by the modified UNIFAC (e.g., those containing piperidinium ILs), experimental data on γ_2^∞ should be used and included in eq 10 instead of $\gamma_2^{\infty, \text{UNIFAC}}$. If such data are not available, the proposed PC-SAFT-UNIFAC calculations cannot be carried out. Besides, the measured data sets of γ_2^∞ versus T are often scattered and are reported in different ranges of temperature. In order to smooth those data and establish a universal γ_2^∞ temperature dependence irrespective of a particular data set, the following relation is recommended

$$\ln \gamma_2^\infty = -\frac{\Delta S_2^{E, \infty}}{R} + \frac{\Delta H_2^{E, \infty}}{RT} \quad (11)$$

Of course, eq 11 is implied by the Gibbs–Helmholtz equation, $(\partial \ln \gamma_2^\infty / \partial T^{-1})_p = \Delta H_2^{E, \infty} / R$ and $\Delta H_2^{E, \infty}$ and $\Delta S_2^{E, \infty}$ stand for average infinite dilution partial excess thermodynamic functions. They can be readily obtained from linear regression of $\ln \gamma_2^\infty$ data as a function of $1/T$.

It is worth noticing that erroneous modified UNIFAC predictions of γ_2^∞ (and thus k_{12}^X) may affect the accuracy of calculations of other properties, e.g., phase equilibria. To estimate that influence, we will provide a comparison of the results of calculations in terms of the PC-SAFT-UNIFAC methodology described above with the PC-SAFT calculations adopting $k_{12}^X(T)$ fitted to the experimental γ_2^∞ temperature dependence given in eq 11.

RESULTS AND DISCUSSION

In the present section, the results of calculations of various thermodynamic properties of pure $[\text{NTf}_2]$ -based ILs as well as binary systems {IL + alkane, cycloalkane, alkene, ketone, ether, alcohol, water} are reviewed and summarized. In particular, we will discuss whether the proposed PC-SAFT-UNIFAC approach is capable of capturing diverse structural effects governing the bulk-phase equilibrium properties. First, the PC-SAFT parametrization is presented for homologous series of 1-alkyl-3-methylimidazolium, 1-alkylpyridinium, 1-alkyl-1-methylpyrrolidinium, and 1-alkyl-1-methylpiperidinium ILs. The full list of names and chemical structures of the considered ILs is presented in the Supporting Information, Table S1. Respective abbreviations used in this paper are $[\text{C}_n\text{C}_1\text{Im}][\text{NTf}_2]$,

$[\text{C}_n\text{Py}][\text{NTf}_2]$, $[\text{C}_n\text{C}_1\text{Pyr}][\text{NTf}_2]$, and $[\text{C}_n\text{C}_1\text{Pip}][\text{NTf}_2]$, where n varies from 1 (methyl) to 14 (n -tetradecyl). Then, the liquid density, vapor pressure, critical properties, and surface tension for the pure ILs were calculated and compared with available experimental/simulation data. The results of calculations of VLE, LLE, SLE, and H^E for binary mixtures composed of IL and nonpolar, or polar, or self-associating solvent are presented in distinct subsections. The molecular components parameters for PC-SAFT are listed in the Supporting Information, Table S2. All of the mixtures' properties were calculated with accordance to the three different procedures in order to underline benefits and shortcomings as well as to specify the range of applicability of the proposed PC-SAFT-UNIFAC approach:

- the classical PC-SAFT predictions, i.e., $k_{12}^X = 0$ (conventional use of LB, WS, and KS combining rules; see eqs 2–4);
- the calculations based on k_{12}^X adjusted to smoothed experimental data, see eq 11 (only if experimental data on γ_2^∞ are available; of course, this procedure it is not purely predictive due to utilization of experimental binary data);
- the PC-SAFT-UNIFAC calculations based on k_{12}^X obtained from eq 9 (only if appropriate UNIFAC representations exist for both IL and solute; in turn, this procedure can be referred to as totally predictive because experimental binary data are not required for calculation of the corrections—the only data required are pure fluid parameters of the mixture's components for the PC-SAFT and their chemical structures for the UNIFAC group assignments).

Let us emphasize that the modified UNIFAC reproduces very accurately the experimental γ_2^∞ for a variety of binary systems, including almost all systems considered in this paper. Therefore, an overview presented in the further text is focused on comparison between approaches (i) and (iii), whereas the results obtained using approach (ii) are recapitulated in detail in the Supporting Information.

Pure Ionic Liquids. The pure fluid PC-SAFT parameters for ILs were obtained by fitting the model predictions to experimental liquid density data extracted from the literature.^{26,27,79–95} Depending on the cation family of ILs, different schemes of calculations were adopted to get and evaluate the PC-SAFT parameters. The general procedure rests on adjusting the physical parameters (m , σ , and u/k_B) to available experimental data on density for a few ILs selected from a given homologous series. The parameters related to self-association, namely, ϵ^{AB}/k_B and κ^{AB} , are fitted together with the physical parameters only for a representative IL of a particular series. Then, it is assumed that the alkyl chain length of the cation does not affect the strength of the associating bonds, and thus, the same values of ϵ^{AB}/k_B and κ^{AB} are assigned to all ILs in the series. The number of segments m and “combined” parameters $m\sigma^3$ and mu/k_B correlate very well with the molar mass (M), and the following linear equations can be set up

$$Y = a + b \times M / (\text{g} \cdot \text{mol}^{-1}), Y = m, m\sigma^3 / \text{\AA}^3, mu / k_B / \text{K} \quad (12)$$

Equation 12 is eventually used to calculate (interpolate/extrapolate) the physical parameters for the ILs not taken into consideration in the optimization procedure mentioned above. Such predicted parameters are evaluated by calculation of liquid

Table 1. Self-Association Parameters for the Four Investigated Families of ILs and the Coefficients for Eq 12 Expressing Molecular Weight Dependence of m , σ , and u/k_B Pure Fluid PC-SAFT Parameters

ILs series	coefficients for eq 12				self-association parameters		%AARD of ρ , see eq 13	
	Y	a	b	R^2	ϵ^{AB}/k_B (K)	κ^{AB}	correlation set	prediction set
$[C_nC_1Im][NTf_2]$ ^{79–86}	m	−0.92945	0.023543	0.9995	2278.41	0.0154	0.09	0.16
	$m\sigma^3/\text{\AA}^3$	−376.4	2.0018	0.9999				
	$mu/k_B/K$	−1693.3	10.552	0.9994				
$[C_nPy][NTf_2]$ ^{87–89,91}	m	−3.0276	0.026519	0.9993	2128.33	0.0217	0.12	0.24
	$m\sigma^3/\text{\AA}^3$	−359.473	1.9626	0.9997				
	$mu/k_B/K$	−1823.8	10.349	0.9994				
$[C_nC_1Pyr][NTf_2]$ ^{92–94}	m	0.0092582	0.019099	0.9922	2089.78	0.0332	0.14	0.95
	$m\sigma^3/\text{\AA}^3$	−398.71	2.07879	0.9998				
	$mu/k_B/K$	−2198.3	10.867	0.9944				
$[C_nC_1Pip][NTf_2]$ ^{26,27,92,95}	m	0.43998	0.019913		1912.10	0.0573	0.28	0.31
	$m\sigma^3/\text{\AA}^3$	−356.42	1.9123					
	$mu/k_B/K$	−1717.9	8.8149					

densities and comparison of the obtained values with corresponding experimental data.

The resulting PC-SAFT parameters (both optimized and interpolated/extrapolated) are listed in the Supporting Information (Table S3), whereas Table 1 summarizes the coefficients a and b from eq 12, self-association parameters describing all four cation families studied and average absolute relative deviations (%AARD) of density defined as

$$\%AARD = \frac{\sum_i |\rho_i^{\text{calcd}} - \rho_i^{\text{exptl}}| / \rho_i^{\text{exptl}}}{N} \times 100 \quad (13)$$

where the summation goes over all data points for all ILs of a given series. Representative results of P – ρ – T calculations for imidazolium ILs, including correlations and predictions at both ambient and elevated pressure, are shown in Figure 1. The procedures and results are discussed in detail in the further text for each series of ILs individually.

For the most common imidazolium series ($[C_nC_1Im][NTf_2]$ with $n = 1–10, 12, 14$) the parameters m , σ , and u/k_B were obtained for odd-numbered imidazolium ILs ($n = 1, 3, 5, 7, 9$). The parameters related to self-association of IL, namely, ϵ^{AB}/k_B and κ^{AB} (see Table 1), were optimized together with m , σ , and u/k_B using density data for $[C_3C_1Im][NTf_2]$. To test the performance of eq 12, the m , σ , and u/k_B parameters for the even-numbered imidazolium ILs were calculated and respective experimental data on liquid density were reproduced by the PC-SAFT equation of state. On the basis of the values of %AARD presented in Table 1, we conclude that the accuracy of correlation and prediction is closely the same. It confirms the internal consistency of the utilized experimental data as well the reliability and applicability of the optimized parameters in interpolating and extrapolating of pure fluid parameters within imidazolium series of $[NTf_2]$ -based ILs.

A similar procedure was adopted for $[C_nPy][NTf_2]$ ($n = 2–5, 6, 8, 10, 12$), $[C_nC_1Pyr][NTf_2]$ ($n = 3–8, 10$), and $[C_nC_1Pip][NTf_2]$ ($n = 3–8$) ILs. However, those classes of ILs were not described in the literature as minutely as the imidazolium series. Only limited data on the density at atmospheric pressure are available for those ILs, and hence, one might expect that the optimized parameters will be not so well behaved as in the case of the imidazolium cation family. In the case of pyridinium ILs, the predictions in terms of eq 12 were performed only for two compounds, viz. $[C_3Py][NTf_2]$ and $[C_5Py][NTf_2]$ with overall %AARD = 0.24, whereas the

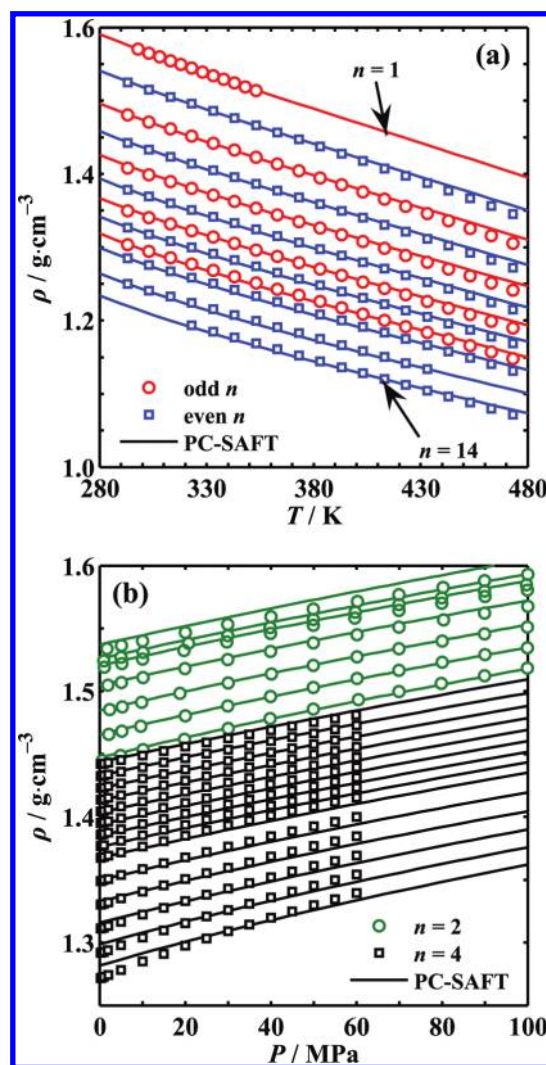


Figure 1. Experimental versus the PC-SAFT calculated P – ρ – T behavior of the imidazolium family of $[NTf_2]$ -based ILs. (a) Atmospheric pressure density for $[C_nC_1Im][NTf_2]$ series ($n = 1–10, 12, 14$): correlations (odd n) and predictions in terms of eqn:mwcorr (even n). Experimental data extracted from the work of Tariq et al.⁸⁰ (b) High-pressure predictions for $[C_2C_1Im][NTf_2]$ and $[C_4C_1Im][NTf_2]$ and comparison with experimental data of Safarov et al.⁸¹ and Nieto de Castro et al.,⁸⁵ respectively.

PC-SAFT parameters were determined by optimization for the remaining ILs with even-numbered side chains attached to the nitrogen atom in the pyridinium cation. Additionally, parametrization of $[\text{C}_4\text{C}_{1(4)}\text{Py}][\text{NTf}_2]$ (where $[\text{C}_4\text{C}_{1(4)}\text{Py}]$ denotes 1-butyl-4-methylpyridinium cation) was performed. The parameters for $[\text{C}_n\text{C}_1\text{Pyr}][\text{NTf}_2]$ ILs with $n = 3, 4, 6, 8$ were obtained from experimental temperature–pressure–density data, and then, their capability of interpolating and extrapolating was tested by calculation of the density of ILs with $n = 5, 7, 10$. In this case, however, the quality of predictions is essentially worse. Finally, the pure fluid parameters for the two first members of the piperdinium cation family (i.e., $[\text{C}_3\text{C}_1\text{Pip}][\text{NTf}_2]$ and $[\text{C}_4\text{C}_1\text{Pip}][\text{NTf}_2]$) were taken from our previous contributions^{26,27} and extrapolated by means of eq 12 in the ILs with longer side chains ($n = 5–8$). One could see that quite accurate predictions were obtained when compared with the experimental densities of Montanino et al.⁹⁵

It is well recognized that one of the key properties of ILs is their extremely low vapor pressure.^{96,97} Therefore, we checked the validity of the parameters listed in Table S3 in the Supporting Information to predict the vapor–liquid equilibrium phase diagrams of some ILs and compared the PC-SAFT calculations with available experimental data. Thus far, the most comprehensive study on the vapor–liquid equilibrium of pure $[\text{NTf}_2]$ -based ILs was reported by Rocha et al.⁹⁸ In this great contribution, the authors presented both an experimental and a theoretical study on the volatility of several imidazolium ILs ($[\text{C}_n\text{C}_1\text{Im}][\text{NTf}_2]$ with $n = 2–8, 10, 12$). The vapor pressure was measured with a new Knudsen effusion apparatus in the temperature range $T = 450–500$ K and confronted with that measured by other authors. Moreover, some important trends between thermodynamic functions of vaporization and the chemical structure of IL were established and confirmed by computer simulations.

On the basis of the phase diagrams plotted in Figure 2, we notice that the PC-SAFT-calculated vapor pressure decreases

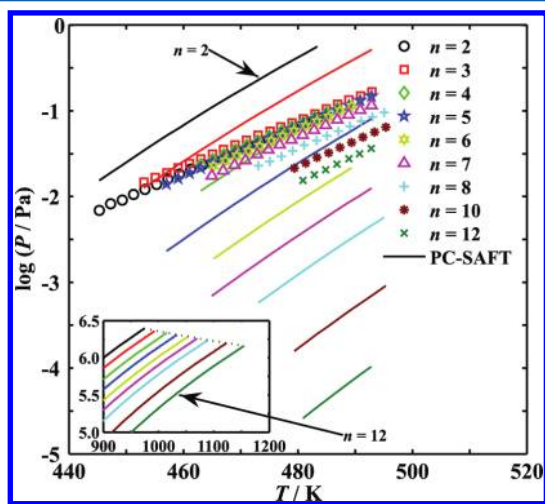


Figure 2. Vapor–liquid equilibrium phase diagrams for pure $[\text{C}_n\text{C}_1\text{Im}][\text{NTf}_2]$ ILs ($n = 2–8, 10, 12$). Points represent experimental data of Rocha et al.⁹⁸ PC-SAFT calculations carried out with the 10-site model of ILs and the parameters listed in Supporting Information, Table S3.

with an increase of the number of carbon atoms in the alkyl chain attached to the imidazolium cation (n). Although this trend is, with some exceptions, in general agreement with

experimental evidence, the observed deviations from experimental data are significant. Due to the low values of observed vapor pressures, %AARD values are very high and vary from 24% for $n = 4$ to 330% for $n = 2$ (see Supporting Information, Table S3). In particular, the calculated vapor pressure is about 1 order of magnitude higher for ILs with shorter side chains ($n = 2, 3$). In turn, for ILs with longer side chains, the predicted vapor pressure is 2 or 3 orders of magnitude lower than experimental ones and the difference between calculated and experimental vapor pressure increases with n . However, we should keep in mind that the measured values are of the range $10^{-3}–10^{-1}$ Pa, and a difference of 2 or 3 orders of magnitude still provides results close to zero. Moreover, the pressure range of results reported in this work covers the pressure range of experimental data. Thus, essential characteristics of ILs are reflected by the incorporated molecular model of ILs. In Figure 2, the critical region for VLE is presented as well for the $[\text{C}_n\text{C}_1\text{Im}][\text{NTf}_2]$ series. We see that the critical temperature increases with n according to PC-SAFT predictions. Unfortunately, this is not in agreement with the results of computer simulations performed very recently by Rai and Maginn.⁴³ In the Supporting Information (Tables S4 and S5) we provide a detailed list of critical temperatures and other properties related to vaporization of pure ILs. Additionally, some of them were compared with respective literature data obtained with different methods.

It is noteworthy that very recently similar calculations were presented with the soft-SAFT equation of state and 3-site molecular model adopted for $[\text{C}_n\text{C}_1\text{Im}][\text{NTf}_2]$ ILs ($n = 2, 4, 6, 8$).³⁴ The authors obtained overestimated values of vapor pressure for all ILs, and the difference was about 1 or 2 orders of magnitude. Furthermore, Rai and Maginn estimated the vapor pressure at $T = 298.15$ K to be in the range 3–6 mPa based on the Monte Carlo simulations carried out at high temperatures (900–1100 K). Of course, this value is rather overestimated as well. On the other hand, the respective vapor pressures obtained from extrapolation of “low-temperature” ($T = 450–500$ K) data of Rocha et al. are on the order of 10^{-9} Pa. We conclude that the proposed 10-site model enhances the vapor pressure predictions for ILs. Let us finally note that the possibility of fitting the molecular parameters to these data was also taken into consideration. However, the idea was discharged because of the absence of a clear pattern for the experimental data and their uncertainty.

To complement characterization of pure ILs in terms of the PC-SAFT coupled with the presented 10-site molecular model, surface tension as a function of temperature was calculated using density gradient theory (DGT).⁹⁹ With accordance to DGT, the vapor–liquid interfacial tension of a pure fluid at temperature T can be expressed as the following integral

$$\gamma(T) = \int_{\rho_V(T)}^{\rho_L(T)} \sqrt{2\kappa[a_0(T, \rho) - \rho\mu_0(T) + P_0(T)]} \, d\rho \quad (14)$$

where $\mu_0(T)$ and $P_0(T)$ are the equilibrium chemical potential and pressure at temperature T and $a_0(T, \rho) = \rho\mu(T, \rho) - P(T, \rho)$ is the Helmholtz free energy density of a homogeneous fluid, whereas $\rho_V(T)$ and $\rho_L(T)$ stand for the orthobaric vapor and liquid number densities, respectively. The parameter κ , the so-called influence parameter, is the characteristic parameter of the DGT. It is usually assumed to be constant or temperature dependent and can be accessed by fitting DGT calculations to the experimental dependency of γ on T . Recently, calculations of γ in terms of the DGT were reported for the imidazolium

series of ILs based on $[\text{NTf}_2]^{34}$ and $[\text{BF}_4]^{37}$ anions with the soft-SAFT equation of state used to represent all thermodynamic properties involved in eq 14. In this study we used PC-SAFT with the 10-site molecular model and parameters listed in Supporting Information, Table S3.

In the case of imidazolium ILs we used the high-temperature data reported recently by the research group of Rebelo⁸⁰ for the $[\text{C}_n\text{C}_1\text{Im}][\text{NTf}_2]$ series, where $n = 2-6, 8, 10, 12, 14$. However, due to significant scatter of those data we applied a linear regression to obtain the smoothed data sets. For $[\text{C}_n\text{Py}][\text{NTf}_2]$ ILs ($n = 2, 4, 5, 6$) the experimental surface tensions were extracted from the papers of Liu et al.,^{88,90} while for the $[\text{C}_n\text{C}_1\text{Pyr}][\text{NTf}_2]$ series the corresponding data reported by Carvahlo et al.¹⁰⁰ ($n = 3, 4$) and Jin et al.¹⁰¹ ($n = 6, 10$) were used. Influence parameters obtained in this work for 17 studied ILs were assumed to be represented as a quadratic function of temperature. The resulting values of the influence parameters as well as the accuracy of correlations expressed as %AARD of the surface tension are tabulated in the Supporting Information, Table S6. The results of calculations are briefly summarized in Figure 3 for $[\text{C}_n\text{C}_1\text{Im}][\text{NTf}_2]$ ($n = 2-8, 10, 12, 14$). Moreover,

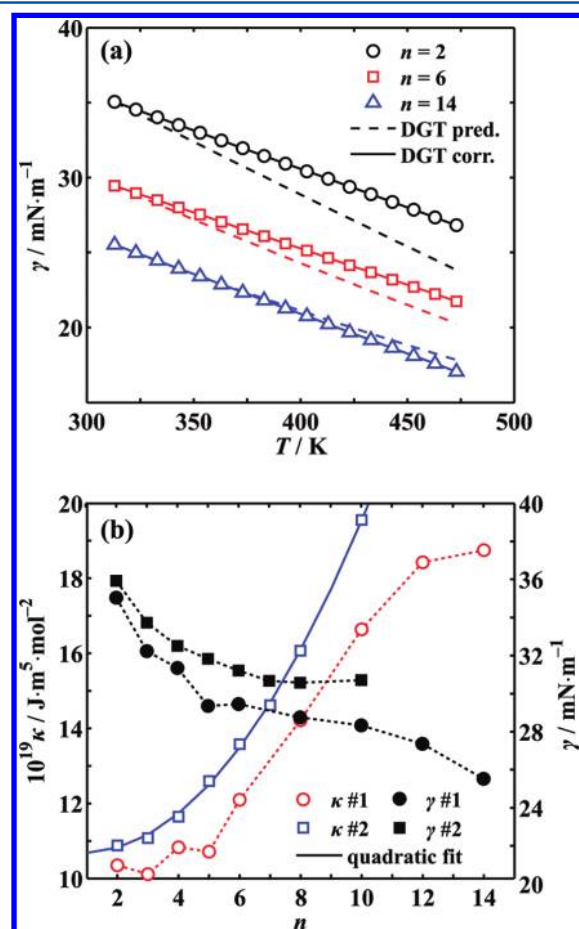


Figure 3. Surface tension (γ) calculations in terms of the density gradient theory (DGT) coupled with the PC-SAFT. (a) Results of calculations for $[\text{C}_n\text{C}_1\text{Im}][\text{NTf}_2]$ series ($n = 2, 6, 14$): calculations with temperature-dependent and -independent influence parameter κ (see details in the text and Supporting Information, Table S6). (b) Experimental γ and calculated κ (at $T = 313.15$ K) as a function of the number of carbon atoms in the cation alkyl side chain (n): comparison of the results obtained based on the data sets of Tariq et al.⁸⁰ and Carvalho et al.¹⁰² (denoted by 1 and 2, respectively).

the results of DGT estimations based on the assumption that κ does not vary with temperature are presented. We see that the general rule for ILs is that γ decreases with the alkyl chain length of the cation, as presented in Figure 3a for some imidazolium ILs. The observed trend is unusual in comparison with common molecular liquids. DGT predicts this kind of behavior providing that κ increases with the length of the alkyl chain of the cation. Furthermore, we see that incorporation of the temperature dependence of κ essentially improves the correlative capabilities of DGT. Moreover, the accuracy of predictions based on a single value of κ is better for ILs with longer side chains. It should be emphasized that the uncertainty of the $\gamma(T)$ experimental data affects the value of the obtained influence parameters. In order to examine that influence, we performed additional calculations for imidazolium ILs using surface tension data measured by Carvalho et al.¹⁰² On the basis of the results shown in Figure 3b one can notice that the revealed $\kappa(n)$ dependence determined from the data of Carvalho et al.¹⁰² can be approximated by a second-order polynomial. In turn, $\kappa(n)$ following from high-temperature data is not so well behaved, which may be related to differences in high- and low-temperature data (within $1.0-2.5$ mN·m⁻¹) and a slightly different scenario from the fairly regular trend exhibited by the low-temperature data.

Binary Systems. A general overview of the range of applicability of the three proposed methodologies and accuracy calculations is shown in Table 2. The calculated data were compared with the respective literature data in terms of %AARD (defined similarly as in eq 13) and average absolute deviation (%AAD) of a given quantity X defined as

$$\%AARD = \frac{\sum_i |X_i^{\text{calcd}} - X_i^{\text{exptl}}| / X_i^{\text{exptl}}}{N} \quad (15)$$

$$\%AAD = \frac{\sum_i |X_i^{\text{calcd}} - X_i^{\text{exptl}}|}{N} \quad (16)$$

Depending on the type of thermodynamic property, X stands for the VLE pressure/temperature, LLE composition (mole fraction of IL), SLE temperature, or excess enthalpy of mixing. For a comprehensive report including detailed information on all systems, including %AARD and %AAD, the reader is referred to the Supporting Information, Tables S6–S9.

{IL + Hydrocarbon} Binary Systems. A great variety of systems discussed in this section were used to investigate the influence of different structural effects of both the ILs and the hydrocarbon molecules on phase behavior (alkyl chain length, cyclic/linear structure, aromaticity, positional isomerism, cation core, and length of the side alkyl chain attached to the cation core). Figure 4 shows the experimental data and results of PC-SAFT-UNIFAC calculations of VLE for a few binary systems containing imidazolium/pyrrolidinium IL and n -alkanes. In Figure 4a the data are summarized for binary systems $\{[\text{C}_6\text{C}_1\text{Pyr}][\text{NTf}_2] + n\text{-hexane}, n\text{-octane}, n\text{-decane}\}$. The resulting PC-SAFT-UNIFAC predictions prove that this approach is able to capture the effect of the alkyl chain length of the hydrocarbon on VLE. Moreover, we see that the model predicts liquid–liquid splitting, and the equilibrium IL-rich phase composition is estimated quite properly compared with the experimental data measured by Nebig et al.⁹⁴ Finally, it should be noticed that the accuracy of VLE and LLE calculations is essentially improved compared with the conventional PC-SAFT predictions ($k_{12}^{\text{LB}} = 0$). In turn, Figure 4b presents

Table 2. Summary of VLE, LLE, SLE, and H^E Calculations in Binary Systems {IL + Molecular Compound} in Terms of the Three Investigated Methods, Namely, Pure PC-SAFT Predictions ($k_{12}^X = 0$), Predictions Based on k_{12}^X Determined from Experimental γ_2^∞ Data, and PC-SAFT-UNIFAC

		%AAD (%AAD) ^a		
data	systems	$k_{12}^X = 0$	k_{12}^X from exptl γ_2^∞	PC-SAFT-UNIFAC
{IL + hydrocarbon} binary systems (X = LB)				
VLE	32	72.3 (13.0)	4.85 (1.70)	4.17 (1.53)
LLE	25	484 (0.303)	55 (0.066)	132 (0.061)
SLE	7	2.91 (7.74)	0.344 (0.925)	
H^E	22	147 (630)	64.7 (227)	28.0 (115)
{IL + polar compound} binary systems (X = KS)				
VLE	11	192 (28.2)	16.4 (5.33)	30.6 (12.0)
LLE	1	265 (0.27)	56.7 (0.02)	
H^E	3	239 (1317)	43.5 (313)	9.21 (64.8)
{IL + alcohol or water} binary systems (X = WS)				
VLE	22	23.1 (5.13)	6.34 (1.60)	5.56 (1.52)
LLE ^b	67	115 (0.233)	86.4 (0.125)	102 (0.178)
SLE	5	0.718 (2.02)	0.285 (0.813)	
H^E	5	80.6 (1073)	13.1 (144)	13.5 (145)

^a%AARD and %AAD denote average absolute relative deviation and average absolute deviation defined in eqs 15 and 16, respectively. %AAD is expressed in the following units: VLE pressure (kPa) or temperature (K), excess enthalpy of mixing ($\text{J}\cdot\text{mol}^{-1}$), SLE temperature (K), LLE IL mole fraction (–). ^bComplete miscibility exhibited by 23 binary systems when $k_{12}^{\text{LB}} = k_{12}^{\text{WS}} = 0$. Those systems were not included in %AARD and %AAD.

the VLE phase diagrams of the systems composed of $[\text{C}_2\text{C}_1\text{Im}][\text{NTf}_2]$ and different hydrocarbons composed of six carbon atoms, viz. *n*-hexane, cyclohexane, cyclohexene, and benzene, at $T = 353.15$ K. We see that the PC-SAFT-UNIFAC predictions are in excellent agreement with experimental data.⁸⁷ Moreover, they are improved compared with the pure predictions, especially in the case of the system with benzene. On the basis of those representative phase diagrams, we conclude that the PC-SAFT-UNIFAC and the 10-site molecular models are capable of providing a good description of the effect on phase equilibria related to the cyclization and aromaticity of the hydrocarbons. Binary isothermal VLE diagrams of systems $\{[\text{C}_n\text{C}_1\text{Im}][\text{NTf}_2] + \text{cyclohexane}\}$ ($n = 1, 2, 4, 6$) were calculated and compared with experimental data^{87,103} to check whether the influence of the alkyl side chain of the imidazolium cation on VLE can be correctly captured by the PC-SAFT-UNIFAC methodology. The results of those calculations are shown in Figure 4c. We conclude that assuming $k_{12}^{\text{LB}} = 0$ provides the results which are only in qualitative agreement with experimental phase diagrams. In turn, application of modified UNIFAC for calculation of the binary corrections yields a more reliable reproducing of both VLE and LLE. Finally, Figure 4d

presents four calculated binary VLE isotherms of system $\{[\text{C}_4\text{C}_1\text{Im}][\text{NTf}_2] + \text{benzene}\}$ and the corresponding experimental data^{87,104} at $T = 298.15$ – 353.15 K. Again, we observed significant improvement in the accuracy of calculations when the PC-SAFT-UNIFAC methodology was employed.

Some representative SLE/LLE calculations for $\{[\text{C}_n\text{C}_1\text{Im}][\text{NTf}_2] + n\text{-alkylbenzene}\}$ ($n = 2, 4, 6, 8, 10$) and $\{[\text{C}_4\text{C}_{1(4)}\text{Py}][\text{NTf}_2] + n\text{-alkylbenzene}\}$ systems are presented in Figure 5 together with corresponding experimental data.^{105–108} The systems studied are particularly interesting due to their unusual LLE phase behavior. We can see in Figure 5a that as the imidazolium alkyl chain length of the IL increases, the behavior of the mixtures containing benzene evolve from a rarely found high-temperature demixing behavior with a lower critical solution temperature (LCST) to the common phase diagram with upper critical solution temperature (UCST). Although the pure prediction describes qualitatively the effect of alkyl chain on the solubility of benzene in imidazolium ILs, the predicted solubilities are much lower than those measured by Łachwa et al.¹⁰⁵ However, when binary interaction parameters k_{12}^{LB} calculated with eq 10 are included in modeling, the results are substantially enhanced. In particular, the unusual phase behavior is captured by the proposed model as well. For $[\text{C}_8\text{C}_1\text{Im}][\text{NTf}_2]$ and $[\text{C}_{10}\text{C}_1\text{Im}][\text{NTf}_2]$ the UCST type of phase diagram is predicted, while for ILs with shorter alkyl chains the “hour-glass” shape of the LLE coexistence curve is reproduced by PC-SAFT-UNIFAC. Unfortunately, the model does not predict the LCST behavior for binary systems $\{[\text{C}_2\text{C}_1\text{Im}][\text{NTf}_2] + n\text{-alkylbenzene}\}$, see Figure 5b. Again, the purely predicted solubilities are much lower than those coming out from the PC-SAFT-UNIFAC calculations. Experimental versus the PC-SAFT-calculated SLE and LLE phase envelopes in binary systems $\{[\text{C}_4\text{C}_{1(4)}\text{Py}][\text{NTf}_2] + \text{benzene, toluene, or ethylbenzene}\}$ are shown in Figure 5c and 5d. The representation of the $[\text{C}_4\text{C}_{1(4)}\text{Py}]^+$ cation is not possible in terms of the modified UNIFAC, and hence, the binary corrections were adjusted to experimental γ_2^∞ data measured by Domańska and Marciniak.¹⁰⁹ As one can easily note, the calculated and experimental phase diagram (including LLE binodal curve, SLE liquidus curves and eutectic point) are in excellent agreement in the case of the system with benzene. Moreover, LCST behavior is captured by PC-SAFT in the systems with other alkylbenzenes. The resulting LLE compositions are, however, slightly overestimated, and the difference between experimental and calculated mole fractions seems to correspond to approximately one methylene group of the side chain of alkylbenzene (i.e., predicted sol. of toluene \approx experimental sol. of ethylbenzene, and so on).

Finally, H^E for some binaries {IL + hydrocarbon} are presented in Figure 6. Experimental^{87,110} and calculated H^E for systems containing $[\text{C}_n\text{C}_1\text{Im}][\text{NTf}_2]$ ILs ($n = 2, 4, 6$) and *n*-hexane are summarized in Figure 6a. We can see that the PC-SAFT equation of state is able to predict both the positive sign of H^E across the whole range of concentration of IL and the trend of H^E against *n*, i.e., $H^E(n = 2) < H^E(n = 4) < H^E(n = 6)$. PC-SAFT-UNIFAC predictions are more accurate in the range of concentration at which IL and *n*-hexane form a single-phase system. However, the predicted H^E values at LLE composition of the IL-rich phase are lower than those revealed by measurements. A completely different dependence of H^E on the mole fraction of IL for $\{[\text{C}_n\text{C}_1\text{Im}][\text{NTf}_2] + \text{benzene}\}$ ($n = 2, 4, 6$) binary systems was revealed by calorimetric measurements of Nebig et al.¹¹⁰ Experimental data are presented in Figure 6b

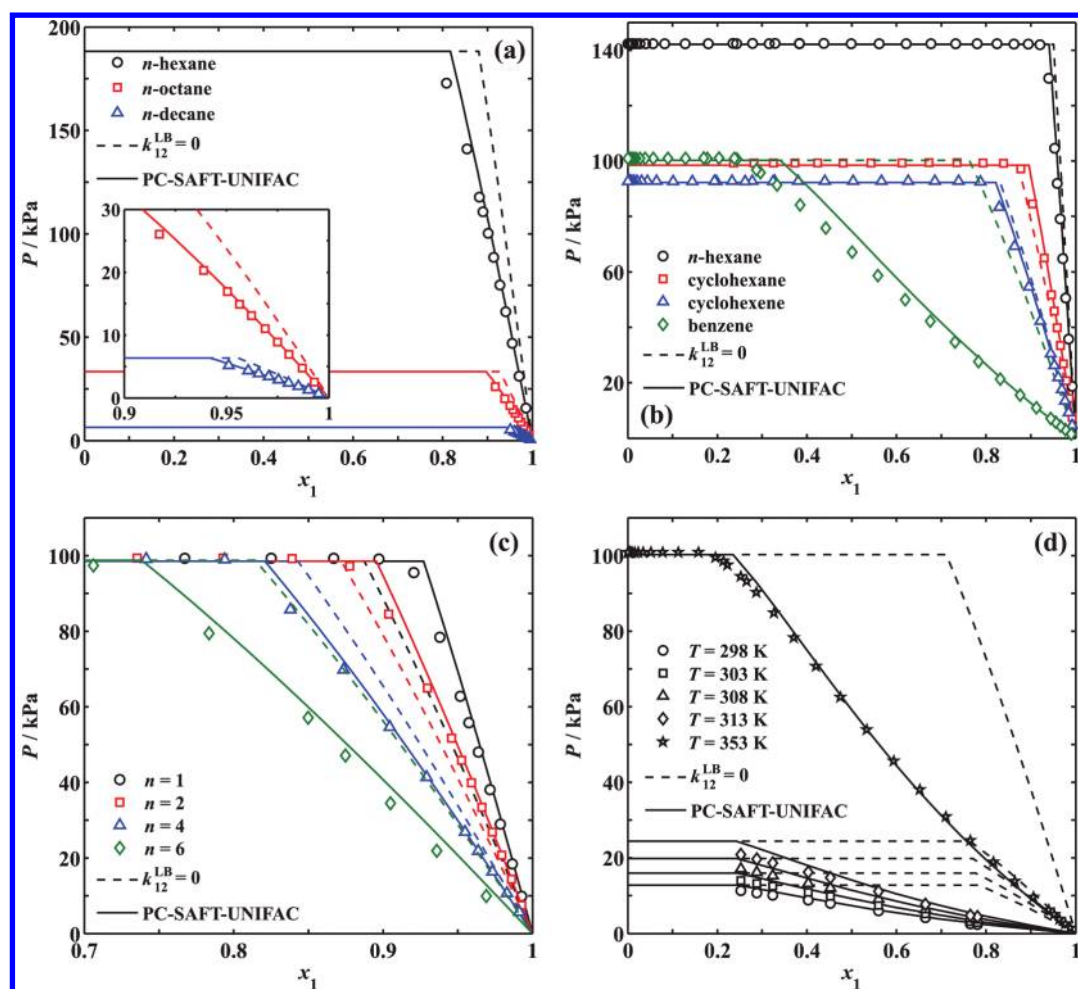


Figure 4. Experimental versus calculated VLE phase diagrams for imidazolium or pyrrolidinium ILs (1) with hydrocarbons (2). (a) Influence of the length of the hydrocarbon chain on VLE: {[C₆C₁Pyr][NTf₂] + *n*-alkane} at *T* = 363.15 K.⁹⁴ (b) Influence of the chemical nature of hydrocarbon on VLE: {[C₂C₁Im][NTf₂] + *n*-hexane, cyclohexane, cyclohexene, or benzene} at *T* = 353.15 K.⁸⁷ (c) Influence of the cation alkyl side chain length on VLE: {[C_{*n*}C₁Im][NTf₂] + cyclohexane} at *T* = 353.15 K (*n* = 1, 2, 4, 6).^{87,103} (d) Influence of temperature on VLE: {[C₄C₁Im][NTf₂] + benzene} at *T* = 298.15–353.15 K.^{87,104}

together with the result of calculations. Experimental H^E is negative in the entire range of the IL mole fraction. Such a behavior is fairly predicted by PC-SAFT-UNIFAC. The absolute value predicted enthalpies of mixing are lower than the corresponding experimental data. In turn, $H^E > 0$ in the whole range of the mixture's composition is obtained with the PC-SAFT when the binary corrections are not accounted for.

{IL + Polar Compound} Binary Systems. In the case of the systems containing ketones and THF, we assumed that pure polar compounds may act as proton acceptors in specific interactions. In turn, the strong polarity of acetonitrile ($\mu \approx 4.0$ D) was described as self-association rather than dipole–dipole interactions. The validity of this assumption can be justified by the experimental¹¹¹ and computational¹¹² studies of NMR spectra of pure acetonitrile and its mixtures with a variety of solvents. Moreover, it was remarked that much better results of VLE calculations can be achieved with this approach compared with those based on the assumption of induced association.^{59,113} On the other hand, thiophene was considered as a nonassociating compound because sulfur atoms are much weaker acceptors than oxygen atoms. Unfortunately, the PC-SAFT-UNIFAC approach could not be applied for systems with acetonitrile and thiophene because of the lack of appropriate

interaction parameters of modified UNIFAC. Thus, parameters expressing the IL–acetonitrile cross-association were calculated using eq 6 with k_{12}^{WS} obtained from experimental γ_2^∞ measured by Heintz et al.,¹¹⁴ whereas the cross-dispersive energy corrections k_{12}^{LB} for IL–thiophene pair were adjusted to experimental γ_2^∞ data reported by Domańska and Mariciniak.¹⁰⁹

VLE and LLE of a few binary systems composed of polar compounds and some imidazolium ILs are presented in Figure 7. VLE data sets for {[C₂C₁Im][NTf₂] + THF or acetonitrile} system, including calculations and measurements of Kato and Gmehling et al.¹⁰³ and Safarov et al.,¹¹⁵ are illustrated in Figure 7a and 7b. In the case of a system containing THF, the pure predictions resulted in liquid-phase splitting not observed in experiments, whereas PC-SAFT-UNIFAC predicts the complete miscibility. Nevertheless, the predicted deviations from ideality are much higher than those following from VLE measurements. To ascertain the reason behind those unsatisfactory results, we compared the experimental limiting activity coefficient of THF in [C₂C₁Im][NTf₂] with the respective value obtained from modified UNIFAC. The only available data set is a single data point $\gamma_2^\infty = 0.800$ measured by Kato and Gmehling at *T* = 353.15 K. The conforming value of the binary correction to the KS combining rule is $k_{12}^{KS} = -1.0204$. In turn, modified

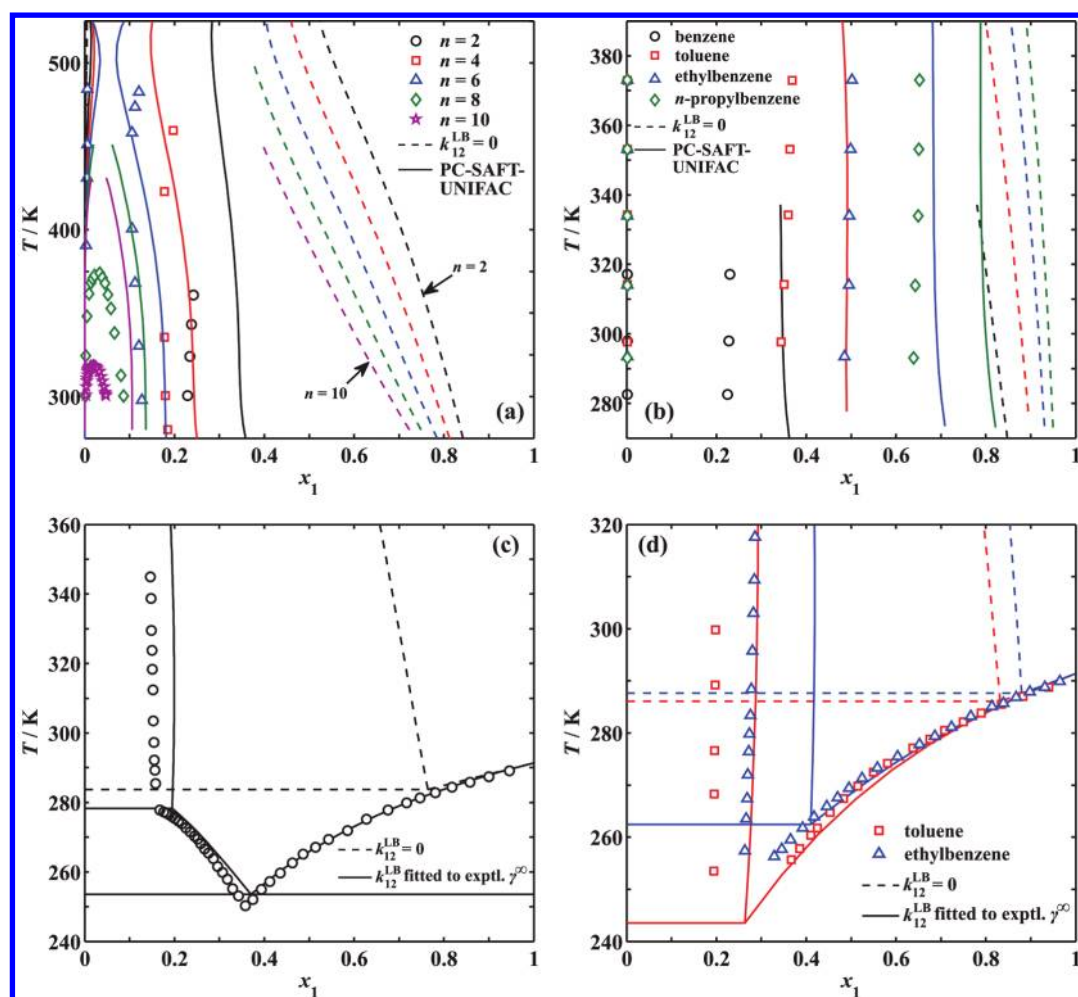


Figure 5. Experimental versus calculated LLE and SLE phase diagrams for imidazolium or pyridinium ILs (1) with *n*-alkylbenzenes (2). (a) Influence of the length of the cation alkyl side chain on LLE: $\{[C_nC_1Im][NTf_2] + \text{benzene}\}$ ($n = 2, 4, 6, 8, 10$).¹⁰⁵ (b) Influence of the length of the alkyl chain of *n*-alkylbenzene: $\{[C_2C_1Im][NTf_2] + \text{benzene, toluene, ethylbenzene, or } n\text{-propylbenzene}\}$.¹⁰⁶ (c) Binary system $\{[C_4C_{1(4)}Py][NTf_2] + \text{benzene}\}$.¹⁰⁸ Predictions based on experimental γ_2^∞ data.¹⁰⁹ (d) Influence of the length of alkyl chain of *n*-alkylbenzene on SLE and LLE: $\{[C_4C_{1(4)}Py][NTf_2] + \text{toluene or ethylbenzene}\}$.¹⁰⁸

UNIFAC calculations give $\gamma_2^{\infty, \text{UNIFAC}} = 0.238$. The resulting value of k_{12}^{KS} is substantially different as well, namely, $k_{12}^{\text{KS}} = -1.3202$. As can be seen in Figure 7a, the results of VLE obtained with the former value of k_{12}^{KS} are improved in comparison with the purely predictive PC-SAFT and PC-SAFT-UNIFAC. Besides, we see that using the single data point of γ_2^∞ (at $T = 353.15$ K) enables correct calculation of the temperature dependence of VLE. Thus, we can draw the conclusion that significant discrepancies between experimental and predicted γ_2^∞ may remarkably affect the PC-SAFT capability of extrapolation from infinite dilution to finite concentrations. Of course, the erroneous results obtained for this particular system follows from the fact that the modified UNIFAC parameters corresponding to interactions between subgroups “THF”, “[C₀C₀Im]”, and “[NTf₂]” were determined based on the limited amount of experimental data.¹⁸ Application of experimental γ_2^∞ for VLE calculations is demonstrated as well for a binary system with acetonitrile as presented in Figure 7b. Finally, the PC-SAFT-calculated LLE phase diagram for a binary system $\{[C_4C_{1(4)}Py][NTf_2] + \text{thiophene}\}$ is presented in Figure 7c and compared with the experimental data points measured by Domańska et al.¹¹⁶ Calculations were performed using uncorrected and corrected LB combining rules adopting

the binary interaction parameters adjusted to experimentally determined γ_2^∞ .¹⁰⁹ Let us note that modeling of this system assuming induced association resulted in complete miscibility. As can be seen in Figure 7c, employment of k_{12}^{LB} fitted to γ_2^∞ enhances the PC-SAFT predictions of IL-rich phase composition. Moreover, the predictions are much better than those obtained from the conventional PC-SAFT calculations, $k_{12}^{\text{LB}} = 0$. The accuracy of the calculations of solubility of the IL in thiophene is improved as well.

Heats of mixing for binary systems $\{[C_nC_1Im][NTf_2] + \text{acetone}\}$ ($n = 4, 6$) and $\{[C_6C_1Im][NTf_2] + \text{acetone, butanone, or 3-pentanone}\}$ at $T = 353.15$ K are shown in Figure 8a and 8b, respectively. As can be seen, the PC-SAFT-UNIFAC calculations are actually in quantitative agreement with experimental data.¹¹⁰ The PC-SAFT predictions with $k_{12}^{\text{LB}} = k_{12}^{\text{KS}} = 0$, however, disclosed completely different behavior, namely, opposite sign of H^E and large miscibility gap increasing with the length of the alkyl chain of the ketone and decreasing with an increase of the alkyl cation alkyl side chain length. Those results confirmed again the wide range of applicability of the proposed PC-SAFT-UNIFAC approach when applied for binary mixtures containing ILs.

{IL + Alcohol or Water} Binary Systems. VLE, LLE, SLE, and H^E calculations for systems {IL + self-associating compound}

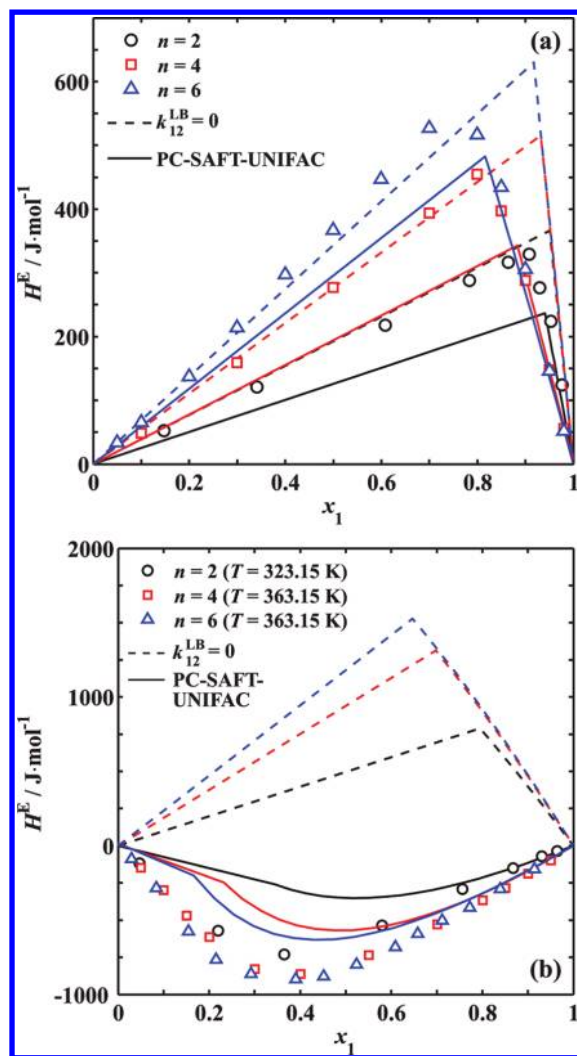


Figure 6. Influence of the cation alkyl side chain on H^E for $[C_nC_1\text{Im}][\text{NTf}_2]$ ILs ($n = 2, 4, 6$) (1) with n -hexane or benzene (2). (a) Binary systems with n -hexane at $T = 363.15$ K.^{87,110} (b) Binary systems with benzene at $T = 323.15$ or 363.15 K.¹¹⁰

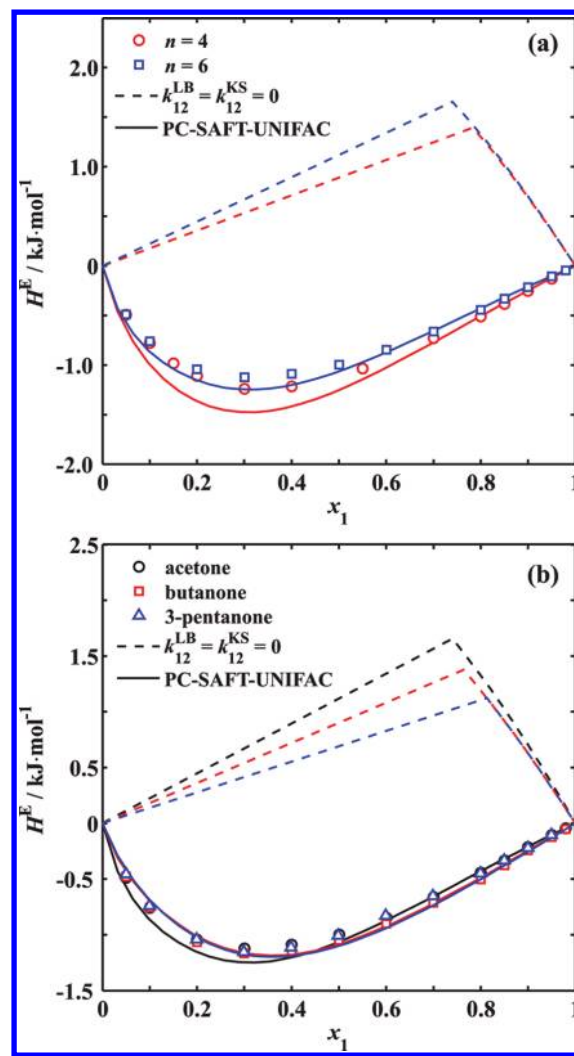


Figure 8. Experimental versus calculated H^E for imidazolium ILs (1) with ketones (2). (a) Influence of the cation alkyl side chain on H^E : $\{[C_nC_1\text{Im}][\text{NTf}_2] + \text{acetone}\}$ ($n = 4, 6$) at $T = 353.15$ K.¹¹⁰ (b) Influence of the alkyl chain length of ketone on H^E : $\{[C_6C_1\text{Im}][\text{NTf}_2] + \text{acetone, butanone, or 3-pentanone}\}$ at $T = 353.15$ K.¹¹⁰

are summarized in this section. The considered compounds are linear alcohols (ranging from methanol to eicosanol), 2-propanol, and water. The calculated phase diagrams are shown in Figures 9–11

and compared with respective experimental data. The pure fluid PC-SAFT parameters for alcohols and water were taken from

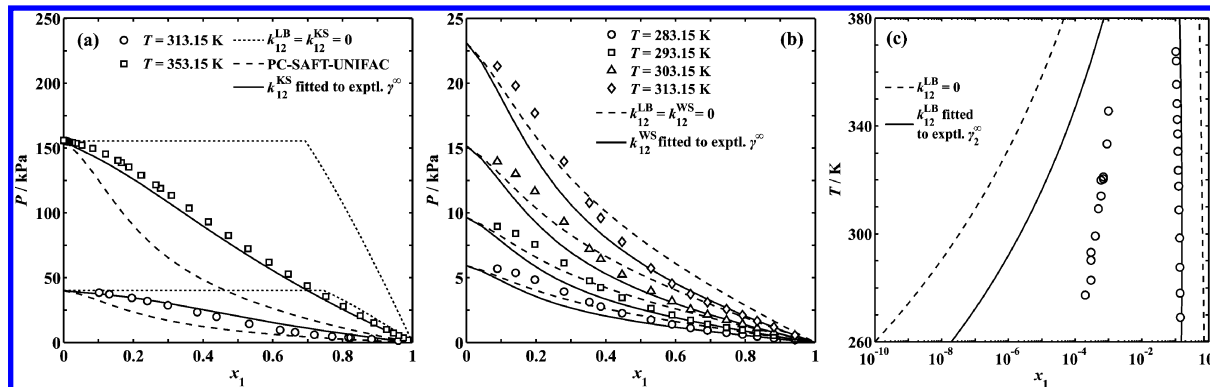


Figure 7. Experimental versus calculated VLE phase diagrams for imidazolium ILs (1) with polar compound (2). (a) VLE in system $\{[C_2C_1\text{Im}][\text{NTf}_2] + \text{THF}\}$ at $T = 313.15$ and 353.15 K.^{103,115} (b) Influence of the temperature of VLE: $\{[C_2C_1\text{Im}][\text{NTf}_2] + \text{acetonitrile}\}$ at $T = 283.15$ – 313.15 K.¹¹⁵ (c) LLE in binary system $\{[C_4C_1(4)\text{Py}][\text{NTf}_2] + \text{thiophene}\}$.¹⁰⁸

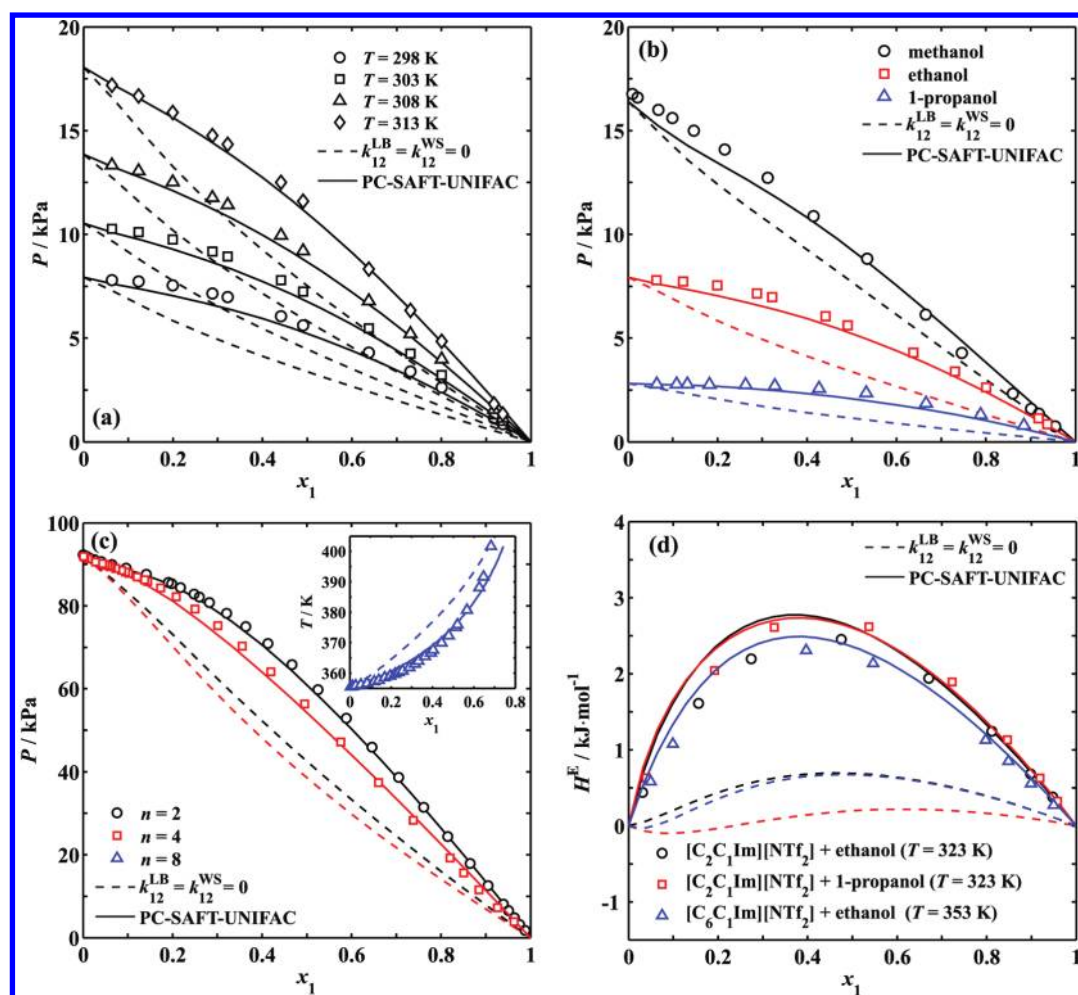


Figure 9. Experimental versus calculated VLE phase diagrams or H^E for imidazolium ILs (1) with alcohols (2). (a) Influence of temperature on VLE: {[C₄C₁Im][NTf₂]} + ethanol at $T = 298.15$ – 313.15 K.¹⁰⁴ (b) Influence of the alkyl chain of the alcohol on VLE: {[C₄C₁Im][NTf₂]} + methanol, ethanol, or 1-propanol at $T = 298.15$ K.¹⁰⁴ (c) Influence of the cation alkyl side chain on VLE: {[C_{*n*}C₁Im][NTf₂]} + 2-propanol at $T = 353.15$ K ($n = 2, 4$) and {[C₈C₁Im][NTf₂]} + 2-propanol at $P = 1$ atm.¹²⁰ (d) Influence of temperature and alkyl chain length of both alcohol and cation on H^E : {[C_{*n*}C₁Im][NTf₂]} + ethanol or 1-propanol ($n = 2, 6$) at $T = 323.15$ and 353.15 K.¹¹⁰

the literature^{46,117} (see Supporting Information, Table S2). Most of the parameters were transferred from the simplified PC-SAFT (sPC-SAFT²) as those parameters are well behaved in terms of eq 12 (thus, they can be extrapolated), and it was shown that they can be successfully used to represent liquid densities and the vapor pressure of a wide variety of alcohols.¹¹⁷ The association scheme adopted for alcohols was 2B according to the Huang–Radosz classification.¹¹⁸ The same model was adopted for water as in the original work of Gross and Sadowski.⁴⁶ Nevertheless, we also checked the performance of other association schemes for H₂O (e.g., four-site scheme 4C adopted recently in soft-SAFT modeling³⁴) and confirmed that the 2B model gives the most accurate predictions of VLE/LLE/SLE when combined with the 10-site model adopted for ILs.

The temperature dependence of the VLE for system {[C₄C₁Im][NTf₂]} + ethanol is presented in Figure 9a, where the results of the PC-SAFT and PC-SAFT-UNIFAC predictions are compared with experimental data reported by Verevkin et al.¹⁰⁴ We see that PC-SAFT predicts negative deviations from Raoult's law when applied in an entirely predictive manner ($k_{12}^{LB} = k_{12}^{WS} = 0$). Those results are in contradiction with experimental data, indicating the positive deviations from ideality, while

the vapor pressure calculated with PC-SAFT-UNIFAC is in excellent agreement with experimental data over the whole range of concentrations of the IL. Figure 9b shows the results of VLE calculations for binary systems {[C₄C₁Im][NTf₂]} + methanol, ethanol, or 1-propanol at $T = 298.15$ K. Again, very promising results were obtained. In particular, PC-SAFT-UNIFAC provides a quantitative description of an influence of the alkyl chain length of the alcohol on VLE. On the other hand, the calculated VLE in binary systems {[C_{*n*}C₁Im][NTf₂]} + 2-propanol ($n = 2, 4, 8$) was compared with experimental data¹¹⁹ to investigate the facility of the PC-SAFT-UNIFAC for capturing the effect of the alkyl side chain of the imidazolium cation, see Figure 9c. Moreover, isobaric VLE at $P = 0.1$ MPa was calculated and compared with the data of Andreatta and co-workers.¹²⁰ On the basis of the results of all those calculations, we conclude that the PC-SAFT-UNIFAC can serve as a powerful tool for prediction of binary VLE in systems composed of imidazolium ILs and alcohols. H^E values in binary systems {IL + alcohol} were calculated and compared with the experimental data of Nebig et al.¹¹⁰ As can be seen in Figure 9d, involving the binary interaction parameters k_{12}^{WS} essentially enhances the calculations and the results are in quantitative agreement with the measured data. When $k_{12}^{LB} = k_{12}^{WS} = 0$, the PC-SAFT calculations

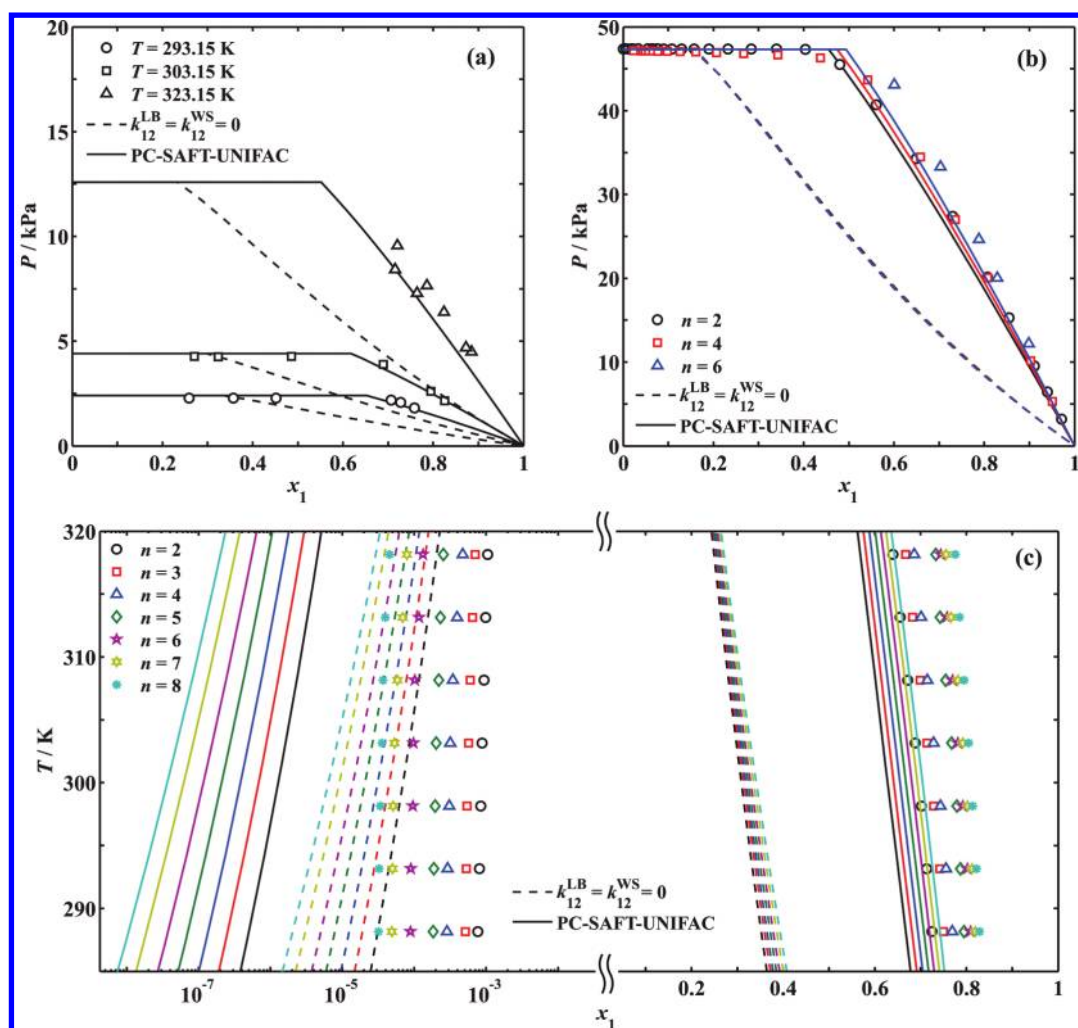


Figure 10. Experimental versus calculated VLE and LLE phase diagrams for imidazolium ILs (1) with water (2). (a) Influence of temperature on VLE: $\{[C_2C_1Im][NTf_2] + \text{water}\}$ at $T = 293.15\text{--}323.15$ K.¹²¹ (b) Influence of cation alkyl chain length on VLE: $\{[C_nC_1Im][NTf_2] + \text{water}\}$ ($n = 2, 4, 6$) at $T = 353.15$ K.^{119,110} (c) Influence of cation alkyl chain length on LLE: $\{[C_nC_1Im][NTf_2] + \text{water}\}$ ($n = 2\text{--}8$).¹²²

result in the heats of mixing which are 1 order of magnitude lower than those evidenced by measurements and in some cases negative or positive depending on the range of mixture composition. In turn, the PC-SAFT-UNIFAC approach predicts positive H^E over the whole range of concentration with a maximum slightly shifted to lower mole fractions of IL. The predicted H^E in the infinite dilution region ($x_2 \rightarrow 0$) agrees very well with experimentally determined values just as the maximum value of H^E (~ 2800 J·mol⁻¹). The former observation confirms the consistency of experimental H^E data with γ_2^∞ data used to determine specific parameters of the modified UNIFAC, whereas the latter one confirms once again the great capability of the proposed approach and molecular models of reliable extrapolating infinite dilution thermodynamic data in finite concentrations.

VLE and LLE in cross-associating mixtures of $[C_nC_1Im][NTf_2]$ ($n = 2\text{--}8$) with water were calculated in the temperature range $T = 288.15\text{--}353.15$ K and compared with available experimental data.^{110,119,121,122} The study on the capability of capturing the temperature dependence and effect of the cation alkyl chain length on isothermal VLE is summarized in Figure 10a and 10b, respectively. Again, the PC-SAFT-UNIFAC approach gives more accurate results than the corresponding pure PC-SAFT predictions. The LLE calculations shown in Figure 10c

follow the same trend as the experimental data, namely, the miscibility gap increases with an increase of the length of the alkyl side chain of the cation. While the results of calculations of the solubility of water in ILs are satisfactory, the predicted compositions of water-rich phase are not. The difference between the predicted and the experimental solubility is even a few orders of magnitude. We believe that this is due to the invalidity of the 10-site molecular model in this range of concentrations. In very dilute aqueous solutions it is more preferable for ILs to exist as ions rather than ion pairs. On the other hand, in more concentrated solutions of ILs (particularly at infinite dilution, i.e., if $x_2 \rightarrow 0$), self-association and ion pairing of ILs prevails over solvation phenomena. Moreover, we observed that the solubility of IL in water calculated assuming $k_{12}^{LB} = k_{12}^{WS} = 0$ is closer to experimental data. In fact, the binary corrections included in eq 6 are positive (see Supporting Information, Table S6). This results in lower values of the cross-association energy and thus decreased mutual affinity of both components of the mixture. Similar results of modeling mutual solubilities of ILs and water were obtained for $[C_4C_1(4)Py][NTf_2]$ and $[C_3C_1Pip][NTf_2]$, see Figure 11. In this case, however, the influence of the cation on the solubility is not predicted correctly compared with experimental evidence.^{108,123}

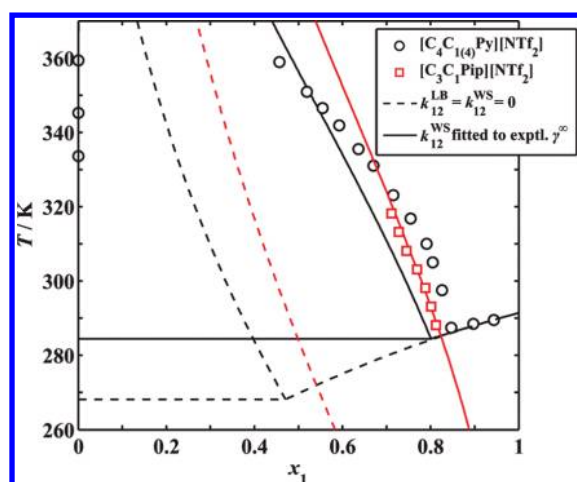


Figure 11. Experimental versus calculated LLE and SLE phase diagrams for $[C_4C_{1(4)}Py][NTf_2]$ and $[C_3C_1Pip][NTf_2]$ (1) with water (2).^{108,123} Pure PC-SAFT predictions compared with calculations adopting k_{12}^{WS} fitted to experimental γ_2^∞ data.¹⁰⁹

CONCLUDING REMARKS

Although the reliability of the proposed PC-SAFT-UNIFAC method was proven for a great number of binary systems, it was shown that in some exceptional cases satisfactory results can be obtained only when experimental data on γ_2^∞ are adopted for calculating the binary corrections. Therefore, we recommend using the PC-SAFT-UNIFAC method only when suitable modified UNIFAC functional groups and reliable parameters are available for the considered systems. If they are not, the experimental data or empirical correlations are preferable.

One might expect that this work should be complemented by a comparison of the results from the proposed PC-SAFT-UNIFAC method with those obtained using the modified UNIFAC. However, it should be emphasized that the modified UNIFAC parameters were obtained by fitting the model predictions to a large number of experimental data points compiled in Dortmund Data Bank (DDB),¹²⁴ and almost all systems and experimental data discussed in this work were employed in the fitting procedure.¹⁸ Thus, one can expect that various thermodynamic properties of ILs-based systems will be reproduced by this model with excellent accuracy. Indeed, it was summarized in numerous papers reported by the research group of Gmehling and confirmed by some preliminary calculations performed in our laboratory. Nevertheless, the following advantages of the method proposed in this work over modified UNIFAC should be highlighted.

- PC-SAFT-UNIFAC is based on an equation of state and a molecular model accounting for some important physical features of ILs, and hence, it provides a more general thermodynamic description (including volumetric and thermodynamic properties of pure components); on the other hand, the reliability of the modified UNIFAC follows from the great correlative capability of this model, large number of model-specific parameters, and large data banks applied for their determination.
- the *only* binary data required to apply the PC-SAFT-UNIFAC approach are the limiting activity coefficients, while the other properties (in general, much harder, more time consuming, and more expensive to measure) are obtained by means of extrapolation from infinite dilution by the PC-SAFT equation of state with the adjusted

binary corrections k_{12}^X , in the case of modified UNIFAC, the binary phase equilibrium data are involved in the parameter determination procedure as well.

It is worth remarking that other models suitable for γ_2^∞ prediction were also considered, e.g., GCM based on a linear solvation energy relationship, developed and evaluated by Mutelet et al.¹²⁵ Finally, the model of Gmehling was chosen due to its wide range of applicability and good correlative capability of γ_2^∞ as a function of temperature and chemical structure of both solute and IL. Although the modified UNIFAC parameters were fitted simultaneously to a comprehensive collection of γ_2^∞ and phase equilibria data sets, we believe that the results summarized in this paper would be approximately the same if the parameters were determined based only on experimental infinite dilution activity coefficients stored in the DDB.

ASSOCIATED CONTENT

Supporting Information

Complete list of names, abbreviations, and structures of ionic liquids considered in this work, tables presenting the PC-SAFT pure fluid parameters for ionic liquids and molecular solvents, detailed report on the accuracy of VLE, LLE, SLE, and H^E calculations, and references for experimental data for binary systems. This material is available free of charge via the Internet at <http://pubs.acs.org>.

AUTHOR INFORMATION

Corresponding Author

*E-mail: kpaduszynski@ch.pw.edu.pl

Notes

The authors declare no competing financial interest.

ACKNOWLEDGMENTS

This work was supported by the European Union in the framework of the European Social Fund through the Warsaw University of Technology Development Programme.

REFERENCES

- Plechokova, N.; Seddon, K. *Chem. Soc. Rev.* **2008**, *37*, 123–150.
- Pereiro, A.; Araujo, J.; Esperanca, J.; Marrucho, I.; Rebelo, L. *J. Chem. Thermodyn.* **2012**, *46*, 2–28.
- Roosen, C.; Müller, P.; Greiner, L. *Appl. Microbiol. Biotechnol.* **2008**, *81*, 607–614.
- Welton, T. *Chem. Rev.* **1999**, *99*, 2071–2084.
- Hallett, J.; Welton, T. *Chem. Rev.* **2011**, *111*, 3508–3576.
- Armand, M.; Endres, F.; MacFarlane, D.; Ohno, H.; Scrosati, B. *Nat. Mater.* **2009**, *8*, 621–629.
- Opallo, M.; Leśniewski, A. *J. Electroanal. Chem.* **2011**, *656*, 2–16.
- Freudenmann, D.; Wolf, S.; Wolff, M.; Feldmann, C. *Angew. Chem., Int. Ed.* **2011**, *50*, 11050–11060.
- Moniruzzaman, M.; Goto, M. *J. Chem. Eng. Jpn.* **2011**, *44*, 370–381.
- Zakrzewska, M.; Bogel-Lukasik, E.; Bogel-Lukasik, R. *Energy Fuels* **2010**, *24*, 737–745.
- Carneiro, A.; Rodriguez, O.; Macedo, E. *Fluid Phase Equilib.* **2011**, *314*, 22–28.
- Xin, Q.; Pfeiffer, K.; Prausnitz, J.; Clark, D.; Blanch, H. *Biotechnol. Bioeng.* **2012**, *109*, 346–352.
- Padmanabhan, M.; Kim, M.; Blanch, H.; Prausnitz, J. *Fluid Phase Equilib.* **2011**, *309*, 89–96.
- Tadesse, H.; Luque, R. *Energy Environ. Sci.* **2011**, *4*, 3913–3929.
- Weingärtner, H. *Angew. Chem., Int. Ed.* **2008**, *47*, 654–670.
- Wendler, K.; Dommert, F.; Zhao, Y.; Berger, R.; Holm, C.; Site, L. *Faraday Discuss.* **2012**, *154*, 111–132.

- (17) Paduszyński, K.; Domańska, U. *Ind. Eng. Chem. Res.* **2012**, *51*, 591–604.
- (18) Nebig, S.; Gmehling, J. *Fluid Phase Equilib.* **2011**, *302*, 220–225.
- (19) Bogel-Lukasik, R.; Matkowska, D.; Bogel-Lukasik, E.; Hofman, T. *Fluid Phase Equilib.* **2010**, *293*, 168–174.
- (20) Domańska, U.; Paduszyński, K. *J. Phys. Chem. B* **2008**, *112*, 11054–11059.
- (21) Domańska, U.; Królikowski, M.; Paduszyński, K. *J. Chem. Thermodyn.* **2009**, *41*, 932–938.
- (22) Domańska, U.; Królikowska, M.; Paduszyński, K. *Fluid Phase Equilib.* **2011**, *303*, 1–9.
- (23) Xu, X.; Peng, C.; Liu, H.; Hu, Y. *Ind. Eng. Chem. Res.* **2009**, *48*, 11189–11201.
- (24) Xu, X.; Peng, C.; Liu, H.; Hu, Y. *Fluid Phase Equilib.* **2011**, *302*, 260–268.
- (25) Tsiptsias, C.; Tsvintzelis, I.; Panayiotou, C. *Phys. Chem. Chem. Phys.* **2010**, *12*, 4843–4851.
- (26) Paduszyński, K.; Chiyen, J.; Ramjugernath, D.; Letcher, T.; Domańska, U. *Fluid Phase Equilib.* **2011**, *305*, 43–52.
- (27) Paduszyński, K.; Domańska, U. *J. Phys. Chem. B* **2011**, *115*, 12537–12548.
- (28) He, C.; Li, J.; Peng, C.; Liu, H.; Hu, Y. *Ind. Eng. Chem. Res.* **2012**, *51*, 3137–3148.
- (29) Rahmati-Rostami, M.; Behzadi, B.; Ghotbi, C. *Fluid Phase Equilib.* **2011**, *309*, 179–189.
- (30) Kroon, M.; Karakatsani, E.; Economou, I.; Witkamp, G.-J.; Peters, C. *J. Phys. Chem. B* **2006**, *110*, 9262–9269.
- (31) Karakatsani, E.; Economou, I.; Kroon, M.; Peters, C.; Witkamp, G.-J. *J. Phys. Chem. C* **2007**, *111*, 15487–15492.
- (32) Andreu, J.; Vega, L. *J. Phys. Chem. C* **2007**, *111*, 16028–16034.
- (33) Andreu, J.; Vega, L. *J. Phys. Chem. B* **2008**, *112*, 15398–15406.
- (34) Llovel, F.; Valente, E.; Vilaseca, O.; Vega, L. *J. Phys. Chem. B* **2011**, *115*, 4387–4398.
- (35) Ji, X.; Adidharma, H. *Chem. Eng. Sci.* **2009**, *64*, 1985–1992.
- (36) Ji, X.; Adidharma, H. *Fluid Phase Equilib.* **2010**, *293*, 141–150.
- (37) Vega, L.; Vilaseca, O.; Llovel, F.; Andreu, J. *Fluid Phase Equilib.* **2010**, *294*, 15–30.
- (38) Maginn, E. *Acc. Chem. Res.* **2007**, *40*, 1200–1207.
- (39) Martín-Betancourt, M.; Romero-Enrique, J.; Rull, L. *J. Phys. Chem. B* **2009**, *113*, 9046–9049.
- (40) Maginn, E. *J. Phys.: Condens. Matter* **2009**, *21*, 373101.
- (41) Leroy, F.; Weiss, V. *J. Chem. Phys.* **2011**, *134*, 094703.
- (42) Méndez-Morales, T.; Carrete, J.; Cabeza, O.; Gallego, L.; Varela, L. *J. Phys. Chem. B* **2011**, *115*, 11170–11182.
- (43) Rai, N.; Maginn, E. *Faraday Discuss.* **2012**, *154*, 53–69.
- (44) Ferreira, A.; Freire, M.; Ribeiro, J.; Lopes, F.; Crespo, J.; Coutinho, J. *Ind. Eng. Chem. Res.* **2011**, *50*, 5279–5294.
- (45) Gross, J.; Sadowski, G. *Ind. Eng. Chem. Res.* **2001**, *40*, 1244–1260.
- (46) Gross, J.; Sadowski, G. *Ind. Eng. Chem. Res.* **2002**, *41*, 5510–5515.
- (47) Gross, J.; Vrabec, J. *AIChE J.* **2006**, *52*, 1194–1204.
- (48) Schacht, C.; Zubeir, L.; de Loos, T.; Gross, J. *Ind. Eng. Chem. Res.* **2010**, *49*, 7646–7653.
- (49) Weidlich, U.; Gmehling, J. *Ind. Eng. Chem. Res.* **1987**, *26*, 1372–1381.
- (50) Gmehling, J.; Li, J.; Schiller, M. *Ind. Eng. Chem. Res.* **1993**, *32*, 178–193.
- (51) Wertheim, M. *J. Stat. Phys.* **1984**, *35*, 19–34.
- (52) Wertheim, M. *J. Stat. Phys.* **1984**, *35*, 35–47.
- (53) Wertheim, M. *J. Stat. Phys.* **1986**, *42*, 459–476.
- (54) Wertheim, M. *J. Stat. Phys.* **1986**, *42*, 477–492.
- (55) Chapman, W.; Gubbins, K.; Jackson, G.; Radosz, M. *Ind. Eng. Chem. Res.* **1990**, *29*, 1709–1721.
- (56) Jog, P.; Chapman, W. *Mol. Phys.* **1999**, *97*, 307–319.
- (57) Karakatsani, E.; Spyriouni, T.; Economou, I. *AIChE J.* **2005**, *51*, 2328–2342.
- (58) Design Institute for Physical Properties, Sponsored by AIChE [2005; 2008; 2009; 2010]. DIPPR Project 801, Full Version. Design Institute for Physical Property Research/AIChE. Online version available at http://knovel.com/web/portal/browse/display?_EXT_KNOVEL_DISPLAY_bookid=1187_VerID=0.
- (59) Grenner, A.; Tsvintzelis, I.; Economou, I.; Panayiotou, C.; Kontogeorgis, G. *Ind. Eng. Chem. Res.* **2008**, *47*, 5636–5650.
- (60) Albers, K.; Sadowski, G. *Ind. Eng. Chem. Res.* **2011**, *50*, 11746–11754.
- (61) Ferrando, N.; de Hemptinne, J.; Mougin, P.; Passarello, J.-P. *J. Phys. Chem. B* **2012**, *116*, 367–377.
- (62) van Westen, T.; Vlugt, T.; Gross, J. *J. Phys. Chem. B* **2011**, *115*, 7872–7880.
- (63) Wolbach, J.; Sandler, S. *Ind. Eng. Chem. Res.* **1998**, *37*, 2917–2928.
- (64) Kleiner, M.; Sadowski, G. *J. Phys. Chem. C* **2007**, *111*, 15544–15553.
- (65) Shimizu, K.; Tariq, M.; Costa Gomes, M.; Rebelo, L.; Canongia Lopes, J. *J. Phys. Chem. B* **2010**, *114*, 5831–5834.
- (66) Tsuzuki, S.; Tokuda, H.; Hayamizu, K.; Watanabe, M. *J. Phys. Chem. B* **2005**, *109*, 16474–16481.
- (67) Katoh, R.; Hara, M.; Tsuzuki, S. *J. Phys. Chem. B* **2008**, *112*, 15426–15430.
- (68) Fernandes, A.; Rocha, M.; Freire, M.; Marrucho, I.; Coutinho, J.; Santos, L. *J. Phys. Chem. B* **2011**, *115*, 4033–4041.
- (69) Weiss, V. C.; Heggen, B.; Muller-Plathe, F. *J. Phys. Chem. C* **2010**, *114*, 3599–3608.
- (70) Canongia Lopes, J.; Padua, A. *J. Phys. Chem. B* **2006**, *110*, 3330–3335.
- (71) Triolo, A.; Russina, O.; Fazio, B.; Appetecchi, G.; Carewska, M.; Passerini, S. *J. Chem. Phys.* **2009**, *130*, 164521.
- (72) Xiao, D.; Hines, L., Jr.; Li, S.; Bartsch, R.; Quitevis, E.; Russina, O.; Triolo, A. *J. Phys. Chem. B* **2009**, *113*, 6426–6433.
- (73) Greaves, T.; Kennedy, D.; Weerawardena, A.; Tse, N.; Kirby, N.; Drummond, C. *J. Phys. Chem. B* **2011**, *115*, 2055–2066.
- (74) Russina, O.; Triolo, A.; Gontrani, L.; Caminiti, R. *J. Phys. Chem. Lett.* **2012**, *3*, 27–33.
- (75) Russina, O.; Triolo, A. *Faraday Discuss.* **2012**, *154*, 97–109.
- (76) Köddermann, T.; Wertz, C.; Heintz, A.; Ludwig, R. *ChemPhysChem* **2006**, *7*, 1944–1949.
- (77) Katsuta, S.; Imai, K.; Kudo, Y.; Takeda, Y.; Seki, H.; Nakakoshi, M. *J. Chem. Eng. Data* **2008**, *53*, 1528–1532.
- (78) Hesse, L.; Sadowski, G. *Ind. Eng. Chem. Res.* **2012**, *51*, 539–546.
- (79) Krummen, M.; Wasserscheid, P.; Gmehling, J. *J. Chem. Eng. Data* **2002**, *47*, 1411–1417.
- (80) Tariq, M.; Serro, A.; Mata, J.; Saramago, B.; Esperanca, J.; Canongia Lopes, J.; Rebelo, L. *Fluid Phase Equilib.* **2010**, *294*, 131–138.
- (81) Safarov, J.; El-Awady, W.; Shahverdiyev, A.; Hassel, E. *J. Chem. Eng. Data* **2011**, *56*, 106–112.
- (82) Esperanca, J.; Visak, Z.; Plechkova, N.; Seddon, K.; Guedes, H.; Rebelo, L. *J. Chem. Eng. Data* **2006**, *51*, 2009–2015.
- (83) Esperanca, J.; Guedes, H.; Canongia Lopes, J.; Rebelo, L. *J. Chem. Eng. Data* **2008**, *53*, 867–870.
- (84) Gardas, R.; Freire, M.; Carvalho, P.; Marrucho, I.; Fonseca, I.; Ferreira, A.; Coutinho, J. *J. Chem. Eng. Data* **2007**, *52*, 1881–1888.
- (85) Nieto de Castro, C.; Langa, E.; Morais, A.; Matos Lopes, M.; Lourenco, M.; Santos, F.; Santos, M.; Canongia Lopes, J.; Veiga, H.; Macatraf, M.; Esperanca, J.; Marques, C.; Rebelo, L.; Afonso, C. *Fluid Phase Equilib.* **2010**, *294*, 157–179.
- (86) Tome, L.; Carvalho, P.; Freire, M.; Marrucho, I.; Fonseca, I.; Ferreira, A.; Coutinho, J.; Gardas, R. *J. Chem. Eng. Data* **2008**, *53*, 1914–1921.
- (87) Kato, R.; Gmehling, J. *Fluid Phase Equilib.* **2004**, *226*, 37–44.
- (88) Liu, Q.-S.; Yang, M.; Li, P.-P.; Sun, S.-S.; Welz-Biermann, U.; Tan, Z.-C.; Zhang, Q.-G. *J. Chem. Eng. Data* **2011**, *56*, 4094–4101.
- (89) Oliveira, F.; Freire, M.; Carvalho, P.; Coutinho, J.; Canongia Lopes, J.; Rebelo, L.; Marrucho, I. *J. Chem. Eng. Data* **2010**, *55*, 4514–4520.
- (90) Liu, Q.-S.; Yang, M.; Yan, P.-F.; Liu, X.-M.; Tan, Z.-C.; Welz-Biermann, U. *J. Chem. Eng. Data* **2010**, *55*, 4928–4930.

- (91) Yunus, N.; Motalib, M.; Man, Z.; Bustam, M.; Murugesan, T. *J. Chem. Thermodyn.* **2010**, *42*, 491–495.
- (92) Gardas, R.; Costa, H.; Freire, M.; Carvahlo, P.; Marrucho, I.; Fonseca, I.; Ferreira, A.; Coutinho, J. *J. Chem. Eng. Data* **2008**, *53*, 805–811.
- (93) Appetecchi, G.; Montanino, M.; Zane, D.; Carewska, M.; Alessandrini, F.; Passerini, S. *Electrochim. Acta* **2009**, *54*, 1325–1332.
- (94) Nebig, S.; Liebert, V.; Gmehling, J. *Fluid Phase Equilib.* **2009**, *277*, 61–67.
- (95) Montanino, M.; Carewska, M.; Alessandrini, F.; Passerini, S.; Appetecchi, G. *Electrochim. Acta* **2011**, *57*, 153–159.
- (96) Esperanca, J.; Canongia Lopes, J.; Tariq, M.; Santos, L.; Magee, J.; Rebelo, L. *J. Chem. Eng. Data* **2009**, *55*, 3–12.
- (97) Ludwig, R.; Kragl, U. *Angew. Chem., Int. Ed.* **2007**, *46*, 6582–6584.
- (98) Rocha, M.; Lima, C.; Gomes, L.; Schroder, B.; Coutinho, J.; Marrucho, I.; Esperanca, J.; Rebelo, L.; Shimizu, K.; Canongia Lopes, J.; Santos, L. *J. Phys. Chem. B* **2011**, *115*, 10919–10926.
- (99) Cahn, J.; Hilliard, J. *J. Chem. Phys.* **1958**, *28*, 258–267.
- (100) Carvalho, P.; Neves, C.; Coutinho, J. *J. Chem. Eng. Data* **2010**, *55*, 3807–3812.
- (101) Jin, H.; O'Hare, B.; Dong, J.; Arzhantsev, S.; Baker, G.; Wishart, J.; Benesi, A.; Maroncelli, M. *J. Phys. Chem. B* **2008**, *112*, 81–92.
- (102) Carvalho, P.; Freire, M.; Marrucho, I.; Queimada, A.; Coutinho, J. *J. Chem. Eng. Data* **2008**, *53*, 1346–1350.
- (103) Kato, R.; Gmehling, J. *J. Chem. Thermodyn.* **2005**, *37*, 603–619.
- (104) Verevkin, S.; Safarov, J.; Bich, E.; Hassel, E.; Heintz, A. *Fluid Phase Equilib.* **2005**, *236*, 222–228.
- (105) Łachwa, J.; Szydlowski, J.; Makowska, A.; Seddon, K.; Esperanca, J.; Guedes, H.; Rebelo, L. *Green Chem.* **2006**, *8*, 262–267.
- (106) Yokozeki, A.; Shiflett, M. *Ind. Eng. Chem. Res.* **2008**, *47*, 8389–8395.
- (107) Shiflett, M.; Niehaus, A. *J. Chem. Eng. Data* **2010**, *55*, 346–353.
- (108) Domańska, U.; Królikowski, M.; Ramjugernath, D.; Letcher, T.; Tumba, K. *J. Phys. Chem. B* **2010**, *114*, 15011–15014.
- (109) Domańska, U.; Marciniak, A. *J. Chem. Thermodyn.* **2009**, *41*, 1350–1355.
- (110) Nebig, S.; Bölts, R.; Gmehling, J. *Fluid Phase Equilib.* **2007**, *258*, 168–178.
- (111) Krestov, A.; Nikiforov, M.; Al'per, G.; Kolker, A. *Russ. Chem. Bull.* **1991**, *40*, 1325.
- (112) Jackowski, K. *Chem. Phys. Lett.* **1992**, *194*, 167–171.
- (113) von Solms, N.; Michelsen, M.; Kontogeorgis, G. *Ind. Eng. Chem. Res.* **2004**, *43*, 1803–1806.
- (114) Heintz, A.; Kulikov, D.; Verevkin, S. *J. Chem. Eng. Data* **2002**, *47*, 894–899.
- (115) Safarov, J.; Geppert-Rybczyńska, M.; Hassel, E.; Heintz, A. *J. Chem. Thermodyn.* **2012**, *56*, 56–61.
- (116) Domańska, U.; Królikowski, M.; Ślesieńska, K. *J. Chem. Thermodyn.* **2009**, *41*, 1303–1311.
- (117) Grenner, A.; Kontogeorgis, G.; von Solms, N.; Michelsen, M. *Fluid Phase Equilib.* **2007**, *258*, 83–94.
- (118) Huang, S.; Radosz, M. *Ind. Eng. Chem. Res.* **1990**, *29*, 2284–2294.
- (119) Kato, R.; Gmehling, J. *Fluid Phase Equilib.* **2005**, *231*, 38–43.
- (120) Andreatta, A.; Arce, A.; Rodil, E.; Soto, A. *Fluid Phase Equilib.* **2010**, *287*, 84–94.
- (121) Husson, P.; Pison, L.; Jacquemin, J.; Costa Gomes, M. *Fluid Phase Equilib.* **2010**, *294*, 98–104.
- (122) Freire, M.; Carvalho, P.; Gardas, R.; Marrucho, I.; Santos, L.; Coutinho, J. *J. Phys. Chem. B* **2008**, *112*, 1604–1610.
- (123) Freire, M.; Neves, C.; Carvalho, P.; Gardas, R.; Fernandes, A.; Marrucho, I.; Santos, L.; Coutinho, J. *J. Phys. Chem. B* **2007**, *111*, 13082–13089.
- (124) Dortmund Data Bank, <http://www.ddbst.de>.
- (125) Mutelet, F.; Ortega-Villa, V.; Moise, J.-C.; Jaubert, J.-N.; Acree, W., Jr. *J. Chem. Eng. Data* **2011**, *56*, 3598–3606.